Coordination Chemistry Reviews, 94 (1989) 67–108
Elsevier Science Publishers B.V., Amsterdam – Printed in The Netherlands

SPIN EQUILIBRIA IN IRON(II) COMPLEXES

H. TOFTLUND

Department of Chemistry, University of Odense, DK 5230 Odense M (Denmark)

(Received 15 July 1988)

CONTENTS

A. ABBREVIATIONS

Abbreviations used for the ligands shown in Schemes 1–4

blbpen	3	L VII	1	$(py)_3$tren	4
bpen	3	ltpen	3	tpa	3
bpmen	3	mbpa	3	tpbn	3
bptn	3	$(mepy)_3$tren	4	tpchxn	3
dpa	2	$(mepy)_2$py tren	4	tpen	3
dppen	1	2-pea	1	tpmbn	3
ebpa	3	phen	1	tppn	3
HBmepz	2	2-pic	1	tptan	4
HBpz	2	ppa	2	tpted	4
iox	1	pyben	1	tpten	4
iptz	1	pyim	1	tptn	4
lbpa	3	pythiaz	2	tp[10]aneN_3	4

0010-8545/89/$14.70

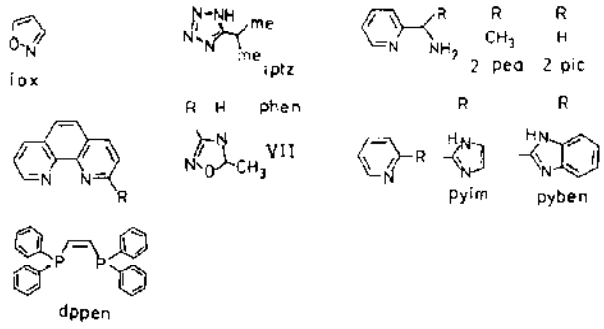

Scheme 1.

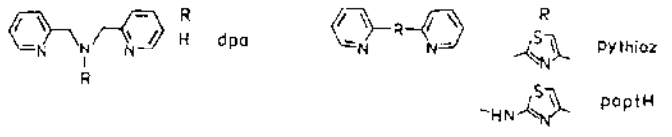

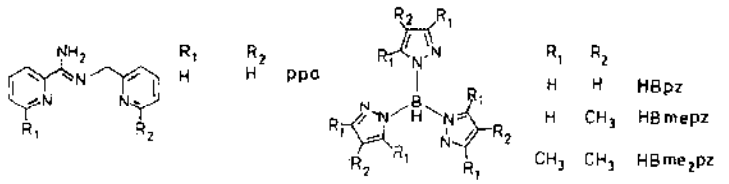

Scheme 2.

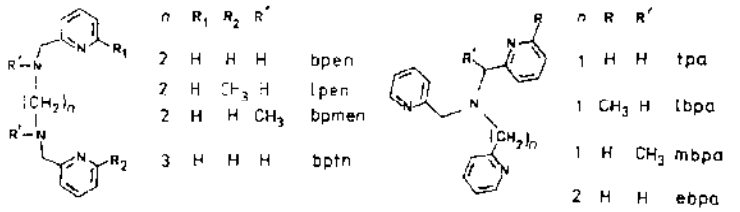

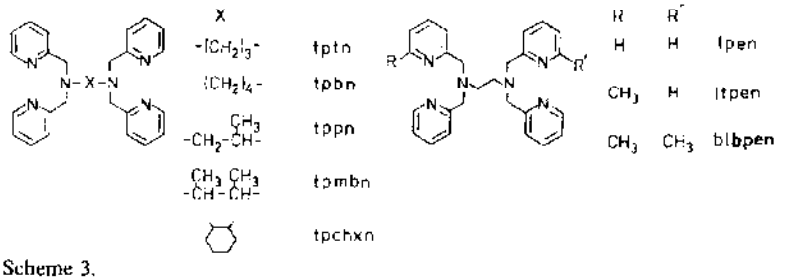

Scheme 3.

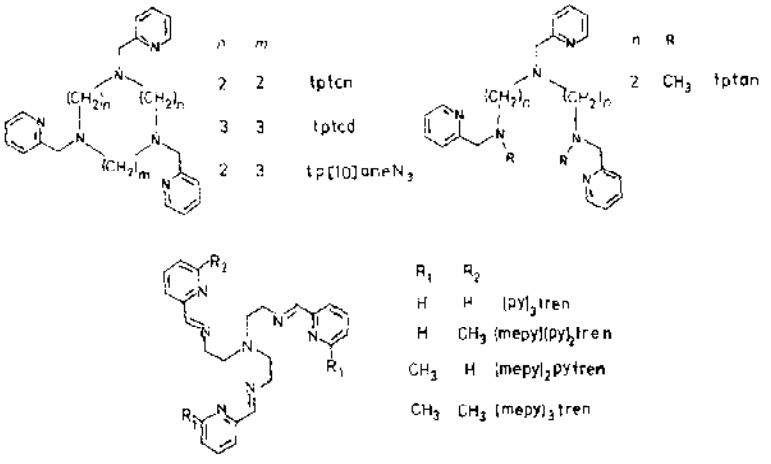

Scheme 4.

A. INTRODUCTION

The first example of an iron(II) spin cross-over system was discovered by Madeja and König [1] in 1963. The phenomenon was, however, predicted by Orgel [2] seven years before the first system was actually characterized. The phenomenon can be observed when the potential minima of the $^1A_1$ and the $^5T_2$ surfaces are so close in energy that both will be thermally populated

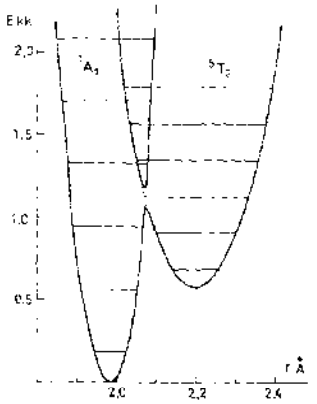

Fig. 1. Potential curves for the two alternative ground states of an iron(II) spin-equilibrium system.

(Fig. 1). The observation of an entropy driven $^1A_1 \rightleftharpoons {}^5T_2$ transformation normally requires that $^1A_1$ is the real ground state.

Today about 50 systems are known, and the field has developed into an important area of contemporary coordination chemistry. Since 1968 there have been a number of review articles covering the subject [3–7]. The review by Gütlich [6] is comprehensive and covers the literature until 1980. About 100 articles have been published in this field since then, and the latest review by König et al. [7] focuses on those which are related to cooperative effects.

The spin-change processes in the solid state have been thoroughly covered by the above reviews. Therefore in the present review I shall mainly focus on contemporary literature which is concerned with the spin-change processes in diluted systems.

As this paper is published in a special issue devoted to coordination chemistry in Denmark, I have found it natural to discuss only the Danish contributions in detail. In the discussion of work done in other groups, topics related to the Danish work have been chosen; it has not been the intention to review the whole field.

B. DESIGN OF NEW SPIN-EQUILIBRIA SYSTEMS

It is natural that the first spin-equilibrium systems were found by accident. However, with 50 systems now known, it is expected that many of these were found as the result of some systematic ligand design, but only in a few cases has such a strategy actually been used. The reason is probably that interest has focused mainly on a very detailed physicochemical description of a few classical examples such as *cis*-$[Fe(phen)_2(NCS)_2]$. Much work has been devoted to the description of the cooperative effects and less attention has been paid to the molecular mechanism of the spin-change processes in diluted systems.

In the following discussion we shall especially refer to systems where spin equilibrium has been established in solution.

Compared with the solid state measurements, measurements on solutions have the advantage that a comparison of the results obtained for related systems can give chemical information about the importance of ligand field effects arising from variations in the substituents in the ligands and from a variation in geometry.

(i) Ligand design

In this section we shall discuss how the spin state of six-coordinate iron(II) complexes depends on the ligand field. In the first approximation we assume that the effective ligand field strength Δ_{oh} is the only relevant

parameter. Later, we shall look at the effects of variations in the interelectronic repulsion and at effects due to distortion of the octahedral symmetry.

Using the parameters introduced in the angular overlap model (AOM) [8] for an MN_6 chromophore, we shall first recall that the observed ligand field splitting Δ^N consists of two contributions:

$$\Delta^N = \Delta^N_\sigma \quad \Delta^N_\pi$$

where Δ^N_σ is due to the overlap between σ orbitals on the ligands and the two $3d$ orbitals on the metal, which in O_h span the e_g set. Δ^N_π arises from the corresponding overlap between π orbitals on the ligands and the three $3d$ orbitals on the metal, which span the t_{2g} set. As the tendency for ammonia and aliphatic amine ligands to engage in π bonds is negligible, we assume that Δ^N_π for these systems is zero. In general, $|\Delta_\sigma| > |\Delta_\pi|$, and for none of the known spin-equilibria systems does $|\Delta^N_\pi|$ exceed 1/5 of Δ^N_σ. For iron(II) imine systems, Δ^N_π values are no doubt negative. Therefore Δ^N tends to be of high value, and complexes of this kind are low spin. However, most iron(II) complexes of aliphatic amine ligands are high spin. (Δ^N_σ alone is not high enough to ensure spin pairing.)

It could be argued that 2-pyridylmethylamine (2-pic) is a good candidate for a ligand giving an intermediate ligand field strength, since it is both an amine and an imine. The ligand field is indeed close to the mean of Δ(bipy) and Δ(en), and the systems $[Fe(2\text{-pic})_3]X_2$ represent examples of spin-equilibria systems [9]. Hancock and McDougall [10] have argued that only conjugated diimines such as bipy should have a sufficiently high $|\Delta^N_\pi|$ and that the ligand field of 2-pic is unusually high. They suggest that complexes of this ligand are stabilized through "hyperconjugation" involving the methylene and the amine groups. A consequence of this hypothesis would be that substitution in the CH_2 or the NH_2 part of 2-pic should stabilize high spin in the corresponding iron(II) complexes.

In order to test this hypothesis we have prepared $[Fe(2\text{-pea})_3](ClO_4)_2$ (2-pea = L(+)-2-pyridyl-1-ethylamine) [11]. Like $[Fe(2\text{-pic})_3](ClO_4)_2$, this system turned out to be a spin-equilibrium system. However, the critical temperatures T_c (the temperature where the amounts of high spin and low spin are equal) are 240 K for the 2-pic system and 100 K for the 2-pea system [11], so this observation supports Hancock and McDougall's hypothesis. Substitution in the NH group of a similar tridentate ligand gives a more convincing trend. $[Fe(dpa)_2]X_2$ (dpa = bis(2-pyridylmethylamine) is low spin, whereas $[Fe(medpa)_2]X_2$ (medpa = *N*-methylbis(2-pyridylmethyl)amine) is high spin in the whole temperature range 77–300 K [12].

Changing the number of chelate rings in the resulting complex offers an alternative possibility for variations in the ligand field strength. Thus we can

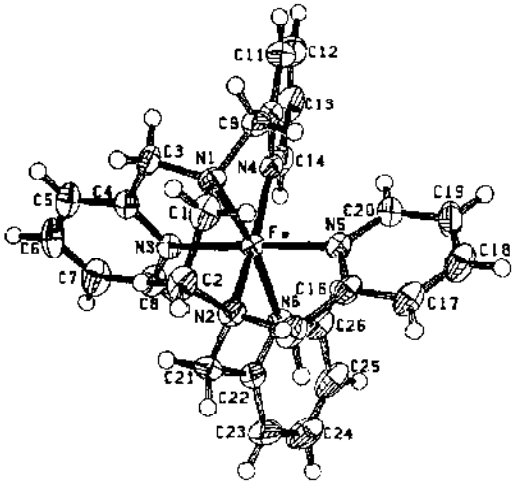

Fig. 2. ORTEP drawing of the molecular structure of the cation in $[Fe(tpen)](ClO_4)_2 \cdot H_2O$ [16].

imagine linking two medpa units together, forming the *N*,*N*,*N'*,*N'*-tetrakis(2-pyridylmethyl)-1,2-ethanediamine (tpen) ligand (Fig. 2). The tpen will bind as a hexadentate ligand, and the resulting complex has five chelate rings which are fused together. In contrast to $[Fe(medpa)_2]X_2$ the $[Fe(tpen)]X_2$ systems are either low spin ($X = PF_6$, BPh_4) or spin-equilibrium ($X = ClO_4^-$) systems [13]; therefore the extra chelate ring has probably increased Δ_o^N so much that it compensates the low Δ_w^N.

That $[Fe(tpen)](ClO_4)_2$ is a spin-equilibrium system was first suggested by Anderegg and Wenk [14]. It was later claimed that the system is pure low spin [15]. The spin-equilibrium properties, however, have now been confirmed both in the solid [13,16] and in solutions [17].

However, even more subtle effects have been observed. When the diamine chelate ring is increased from a five- into a six-membered ring (forming tptn) the resulting iron(II) complex salts are always low spin [13], despite the expected drop in the ligand field strength. In order to explain this variation we suggest that $[Fe(tpen)]X_2$ systems are actually more strained than $[Fe(tptn)]X_2$ systems. Finally, when the diamine chelate is expanded further to a seven-membered ring, the resulting $[Fe(tpbn)]X_2$ complex salts are predominantly high spin [18].

Instead of using steric strain in the design of new systems, another strategy is to introduce steric bulk. Typically a ligand forming a low-spin complex is modified by introducing bulky groups. These prevent the donor atoms from coming so close to the central atom that spin pairing occurs, and

a situation with longer Fe–N bonds is favoured, facilitating a population of antibonding $e_g(d_{z^2}, d_{x^2-y^2})$ orbitals at iron(II). Wilson et al. [19] have used this strategy to modify the low-spin complex $[Fe(Py_3tren)]X_2$ (Py_3tren is the tris Schiff base derived from tris(2-aminoethyl)amine and 2-pyridinecarbaldehyde) by introducing methyl groups in the 6-position of one or two of the pyridine groups. In that way they obtained new spin-equilibria systems. We have used the same strategy on the tpen-type systems. The introduction of just one methyl group forming $[Fe(1tpen)]X_2$ is enough to produce a pure high-spin complex [13].

(ii) Anion and solvent effects

Considering how sensitive the spin states of iron(II) complexes are to steric and inductive effects when Δ is close to the critical value, it is not surprising that the spin state can vary if the counter-ion or the solvent of crystallization is changed.

It seems to be a general trend that polar solvents of crystallization will stabilize the low-spin forms. In a few cases, X-ray diffraction data on different solvates have established the importance of hydrogen bonds.

Thus in the low-spin system, *fac*-$[Fe(2\text{-pic})_3]Cl_2 \cdot 2\ H_2O$, hydrogen bonds are found between H_2O, NH_2 and Cl. The corresponding anhydrous salt is a spin-equilibrium system ($T_c = 110$ K) [20,21]. Strong hydrogen bonds involving NH_2 will increase the σ-donor properties of this group and thus favour low spin.

It has been somewhat more difficult to rationalize the influence of the counter-ions on the spin state. There is no correlation between the size and charge of an anion and the spin state of the salts, so the lattice energy does not seem to contribute significantly to the ligand field. We have examined several salts of the type $[Fe(tpen)]X_2$ (Fig. 3). The halides I^- and Br^- are similar to the PF_6^- case. Only the perchlorate has a T_c (380 K) which is low enough for the system to qualify as a spin-equilibrium system [16]. However, ClO_4^- is neither the largest nor the smallest of the counter-ions investigated.

Sorai et al. [22] have shown that dilution of $[Fe(2\text{-pic})_3]Cl_2 \cdot C_2H_5OH$ into the isomorphous zinc(II) compound gives rise to a gradual decrease in T_c (up to 40 K), when the molar fraction $X(Fe)$ goes from 1.00 to 0.0009. Based on the ionic radii of low-spin iron(II), zinc(II) and high-spin iron(II) being 0.75 Å, 0.88 Å and 0.92 Å respectively, it is expected that dilution favours high spin as the sizes of the zinc(II) host and high-spin(II) complex ions are expected to be very close to each other.

Figure 3 shows the effect on the magnetic moment of diluting $[Fe(tpen)](ClO_4)_2$ into the corresponding zinc(II) complex. In this case, only

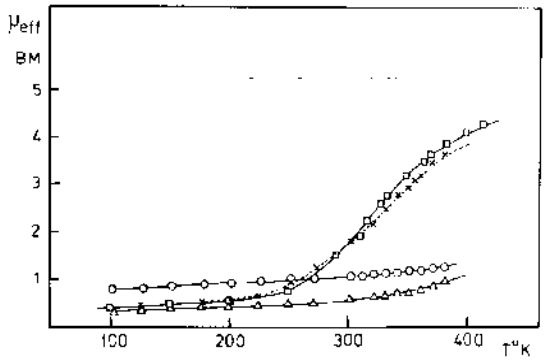

Fig. 3. Magnetic moment as a function of temperature for a series of [Fe(tpen)]X_2 salts [16]: □, X = perchlorate; ×, X = perchlorate, diluted into a zinc(II) host, △, X = hexafluorophosphate; ○, X = tetraphenyl borate.

a very small effect is observed, and in contrast to the 2-pic system it is the low-spin state that is stabilized by dilution [16].

As we shall see in a later section on solution properties, the general trend seems to be that dissolution of a spin-equilibrium system in a liquid solvent changes the equilibrium towards the high-spin side. However, there are exceptions to this rule.

C. CHARACTERIZATION OF SPIN EQUILIBRIA IN THE SOLID STATE

The temperature variation of magnetic susceptibility is the classical and the most direct criterion for spin equilibrium in a solid. Nevertheless, since such a measurement gives a macroscopic description, it cannot be used to prove that two different spin states exist simultaneously. It is therefore essential that susceptibility measurements are supplemented by at least one microscopic criterion.

In the study of spin equilibria in iron(II) and iron(III) systems, Mössbauer spectroscopy has been the preferred technique to provide a microscopic criterion. However, the time resolution of a ^{57}Fe Mössbauer experiment is limited by the lifetime of the excited ^{57}Fe nucleus (6.94×10^{-8} s). If the lifetime of a given spin state is comparable to this figure the lines will broaden or merge owing to relaxation processes.

IR spectroscopy, however, can nearly always be used as a microscopic criterion since the characteristic time scale is of the order of 10^{-11} s, which is shorter than the lifetime of the spin states of any known spin-equilibrium system.

(i) Magnetic susceptibility

In this section we shall attempt to classify a series of spin-equilibria systems according to their behaviour during the spin change process.

In Table 1 the low temperature and the high temperature magnetic moment of 20 systems prepared by our group are presented. In the cases where a critical temperature T_c is defined, it has been cited. Each system has been classified according to the following designations: h or l indicate that the system in question is found predominantly as high spin or low spin respectively over a large temperature range. The designation eq (equilibrium) is used to indicate a system in which the magnetic moment gradually changes over a temperature range of more than 100 K. More abrupt spin transitions are indicated as co (cross-over). If the spin change, for one reason or the other, is not complete, the symbol p (plateau) is used. Finally, m indicates that the system seems to be a mixture of isomers with different spin states which are not in equilibrium.

TABLE 1

Magnetic moments of iron(II) complexes in the solid state

Compound	μ_{eff} (BM)	(T (K))	μ_{eff} (BM)	(T (K))	T_c (K)	Class [a]	Ref.
$[Fe(2\text{-pic})_3](ClO_4)_2$	2.91	100	5.17	350	234	eq, p	11
$[Fe(2\text{-pea})_3](ClO_4)_2$	3.91	100	5.19	300	90	eq, p	11
$[Fe(tptan)](ClO_4)_2$	4.50	106	4.70	409		h	23
$[Fe(tptcn)](ClO_4)_2$	1.20	303	1.26	406		l	23
$[Fe(tpted)](ClO_4)_2$	3.71	107	413	303	100	m, eq	23
$[Fe(tpen)](ClO_4)_2$	0.38	100	4.22	412	380	eq	13
$[Fe(tppn)](ClO_4)_2$	0.97	305	2.37	403	402	eq	13
$[Fe(tpchxn)](ClO_4)_2$	1.15	305	3.05	402	445	eq	13
$[Fe(tpmbn)](ClO_4)_2$	1.16	300				l	18
$[Fe(tptn)](ClO_4)_2$	0.75	300				l	13
$[Fe(tpbn)](ClO_4)_2$	3.77	4	4.73	300		h(eq)	18
$[Fe(ltpen)](ClO_4)_2$	4.70	100	5.08	403		h	13
$[Fe(bpen)(NCS)_2]$	2.35	50	5.42	300	70	co	25
$[Fe(bptn)(NCS)_2]$	1.38	50	5.18	300	170	eq	25
$[Fe(bpmcn)(NCS)_2]$	5.00	70	5.06	300		m, h	25
$[Fe(tpa)(NCS)_2]$	2.83	80	5.46	300	170	co, p	24
$[Fe(tpa)(NCSe)_2]$	1.40	100	4.70	300	232	co	18
$[Fe(tpa)(NCBH_3)_2]$	2.35	90	2.49	300		m	18
$[Fe(mbpa)(NCS)_2]$	2.94	80	5.33	300	130	eq, p	24
$[Fe(ebpa)(NCS)_2]$	4.33	80	4.28	300		m	24

[a] Abbreviations: co, cross-over; eq, equilibrium; h, high spin; l, low spin; m, mixture of isomers; p, plateau.

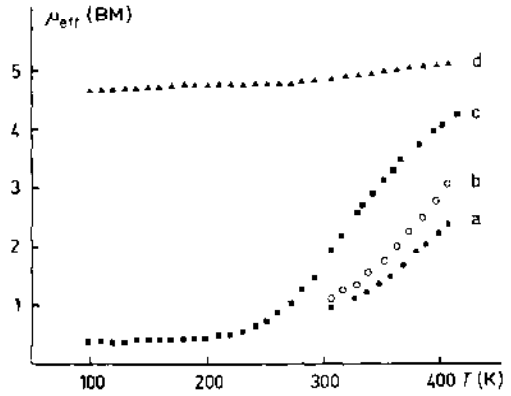

Fig. 4. Temperature dependence of the effective magnetic moments μ_{eff} [13]: (a) [Fe(tppn)]$(ClO_4)_2 \cdot H_2O$, (b) [Fe(tpchxn)]$(ClO_4)_2 \cdot 2\ H_2O$. (c) [Fe(tpen)$(ClO_4)_2 \cdot H_2O$, (d) [Fe(ltpen)]$(ClO_4)_2 \cdot H_2O$.

Among the systems in Table 1, all sorts of abnormal behaviour have been observed, and an unambiguous classification has been difficult. A more detailed picture is obtained from an inspection of some of the experimental μ_{eff} vs. T curves shown in Figs. 4–8.

Even the most gradual spin-equilibria systems seldom follow the expected curve for a Boltzmann distribution among the lowest thermally accessible electronic states. Only those systems for which a simple empirical thermodynamic analysis of the data is satisfactory are designated eq. It is assumed that such systems can be described as an equilibrium among the two states HS and LS ($K = [HS]/[LS]$). If a plot of $\ln K$ against $1/T$ is linear to a good approximation in the whole temperature range, the spin-equilibrium condition is confirmed. Typical examples are [Fe(tpen)]$(ClO_4)_2$ (Fig. 4(c)) and *cis*-[Fe(bptn)$(NCS)_2$] (Fig. 5) [13,25]. The magnetic behaviour of these systems is to a good approximation, the same in the solid as in solution, and it is therefore assumed that a true equilibrium among distinct molecular species exists for these systems.

A typical example of an "abrupt" or cross-over system (co) is *cis*-[Fe(bpen)$(NCS)_2$] (Fig. 5) [25]. In this type of system the spin change process is coupled to a first-order phase transition in the material [7].

Cross-over systems often show thermal hysteresis. Thus the transition temperatures T_c observed on cooling are lower than those observed on heating. In the actual case a change in T_c values of 4 K was observed when cooling from 100 to 4 K was performed over several hours. If the sample is rapidly cooled from room temperature to 4 K, it can be frozen in a state of almost high spin with $\mu_{eff} = 4$ BM. During the subsequent increase in

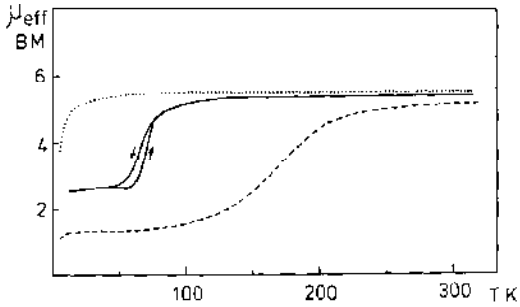

Fig. 5. Temperature dependence of the effective magnetic moments μ_{eff} [25]: .... *cis*-[Fe(blen)(NCS)$_2$]; ——, *cis*-[Fe(bpen)(NCS)$_2$]; — — —, *cis*-[Fe(bptn)(NCS)$_2$].

temperature the moment first increases to about 4.5 BM, then from 50 K it drops to a minimum of 3 BM at 60 K, and finally it follows the regular variation (Fig. 6) [25].

Very recently, two further examples of the freezing of metastable high-spin states have been published [26,27]. In both cases the kinetics of the high-spin to low-spin interconversions were examined. Activation energies of 19.5 kJ mol^{-1} [27] and 30.5 kJ mol^{-1} [26] were found.

The development of plateau or abrupt transitions is only observed for solids, so that an explanation of these phenomena must be found among the specific intermolecular interactions in the crystal lattices in question. Some thermodynamic theories based on lattice properties and which can describe these cooperative effects have been developed [7].

In Fig. 7 the temperature variation of the magnetic moment of [Fe(2-pic)$_3$](ClO$_4$)$_2$ · H$_2$O is shown [11]. The corresponding chloride system is a typical abrupt system showing hysteresis ($T_C^{\downarrow}$, 200 K; $T_C^{\uparrow}$, 300 K) [21], whereas the present system is gradual.

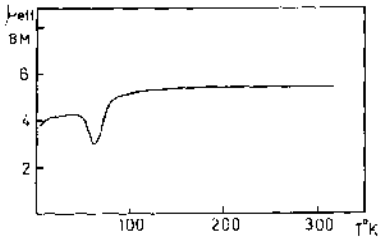

Fig. 6. Magnetic moment μ_{eff} as a function of temperature for the heating of supercooled high-spin *cis*-[Fe(bpen)(NCS)$_2$].

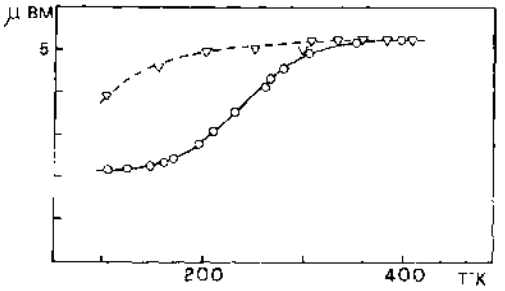

Fig. 7. Temperature variation of the effective magnetic moment [11]: ○, $[Fe(2\text{-pic})_3](ClO_4)_2$; ▽ $[Fe(2\text{-pea})_3](ClO_4)_2$.

Among the systems in Table 1 there are some having a nearly temperature-independent magnetic moment, which corresponds neither to high spin nor to low spin (Fig. 8). There are several possible explanations of this behaviour. The sample might be a mixture of high-spin and low-spin components, or if it is pure, the spin transition might be frozen and the ratio of high spin to low spin is maintained at an intermediate value in the whole temperature range. The obvious possibility that an iron(II) system can have a ground state with an intermediate spin (triplet) has not yet been confirmed [6,7]. In any case the nature of these kinds of systems must be determined with the help of other techniques. Thus, although the magnetic moment of *cis*$[Fe(tpa)(NCBH_3)_2]$ is close to the value expected for a pure triplet state ($\sqrt{8} = 2.83$ BM), the Mössbauer spectra clearly show that the system is a mixture of singlet and quintet forms [18].

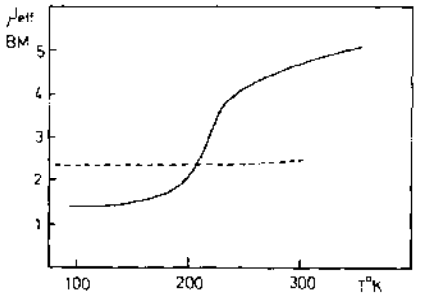

Fig. 8. Temperature variation of the effective magnetic moment [18]: ——, *cis*-$[Fe(tpa)(NCSe)_2]$; · · ·, *cis*-$[Fe(tpa)(NCBH_3)_2]$.

(ii) Mössbauer spectroscopy

The use of Mössbauer spectroscopy in the characterization of spin-equilibria systems goes back to 1966, when this technique was only 8 years old [28]. Several groups have reported ^{57}Fe Mössbauer spectra as a function of temperature for spin-equilibria systems [6,7].

A temperature-induced spin transition is typically seen as a drop in the intensity of the high-spin signal ($\Delta E_Q = 1.5$–3 mm S^{-1}; $\delta \approx 1$ mm s^{-1}) on cooling, at the same time as the low-spin signal ($\Delta E_Q = 0.2$–0.5 mm s^{-1}); $\delta \approx 0.5$ mm s^{-1}) increases. As a rule, both signals can be observed in a certain temperature range around the T_c found from magnetic susceptibility measurements. In collaboration with Trautwein's group we have investigated a long series of compounds prepared by our group. In Table 2 the Mössbauer parameters are given. For the spin-equilibria systems the parameters above and below T_c are given. Some of these systems deviate from the usual pattern. However, the spectra of *cis*-[Fe(bptn)$(NCS)_2$] (Fig. 9) show the expected variation.

In the case of [$Fe_{0.1}Zn_{0.9}$tpchxn]$(ClO_4)_2$ a set of highly unusual spectra is obtained above 200 K (Fig. 10). At 100 K, two doublets can clearly be distinguished, yet at 200 K an additional line is discernible, which may be attributed to a third doublet. The parameters for this third doublet suggest that it arises from an additional quintet state. An obvious explanation could be that the $^5T_{2g}$ state is split owing to a distortion of the ligand field. Fleisch

TABLE 2

Mössbauer parameters for spin-equilibria systems

Compound		∂ (mm s^{-1})	ΔE_Q (mm s^{-1})	T (K)	∂ (mm s^{-1})	ΔE_Q (mm s^{-1})	T (K)
[Fe(tptcd)]$(SbF_6)_2$ [a]	HS	1.074	1.959	120			
	HS	1.021	1.521	120			
[Fe(tptan)]$(SbF_6)_2$	HS	1.06	3.15	4	0.90	2.80	265
[Fe(tptcn)]$(ClO_4)_2$	LS	0.293	0.168	100	0.349	0.176	340
[Fe(bptn)$(NCS)_2$] [b]	HS	1.053	2.442	170	0.963	2.165	225
	LS	0.463	0.298	170	0.3	0.4	225
[Fe(tpen)]$(PF_6)_2$ [c]		0.359	0.493	240	0.363	0.478	340
[Fe(tpen)]$(ClO_4)_2$		0.365	0.543	120	0.482	0.352	350
[Fe(tpchxn)]$(ClO_4)_2$		0.46	0.42	77	0.30	0.41	300
[Fe(tpbn)]$(ClO_4)_2$ [d]	HS	1.08	2.84	4	1.00	2.67	220
	LS	0.51	0.35	4		–	220
[Fe(tpa)$(NCBH_3)_2$]	HS	0.83	3.22	50			
	LS	0.20	0.38	50			

[a] Ref. 23. [b] Ref. 29. [c] Ref. 16. [d] Ref. 18.

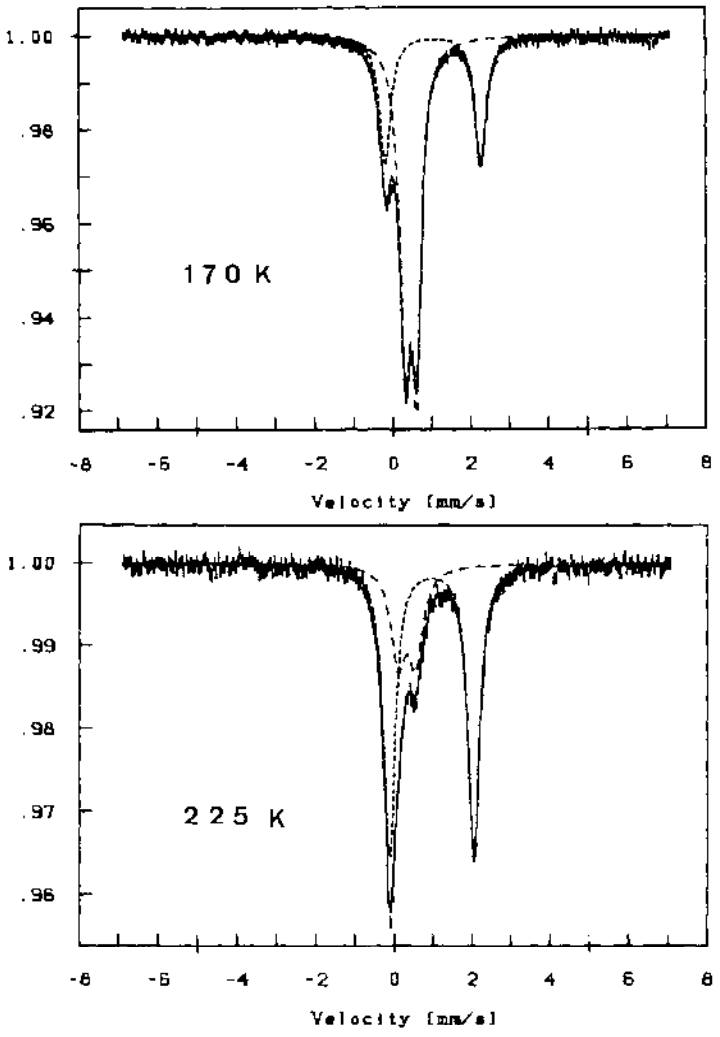

Fig. 9. Experimental Mössbauer spectra of *cis*-[Fe(bptn)$(NCS)_2$] with solid lines representing HS and LS quadrupole doublets, which have been obtained by a least-squares fit using Lorentzians [29].

et al. [30] have observed similar behaviour for [Fe(2-CH_3-phen)$_3$]$(ClO_4)_2$. At elevated temperatures the lines broaden and tend to merge, which is characteristic for relaxation processes. A requirement for the observation of this phenomenon is that the spin interconversion rate is comparable with the rate

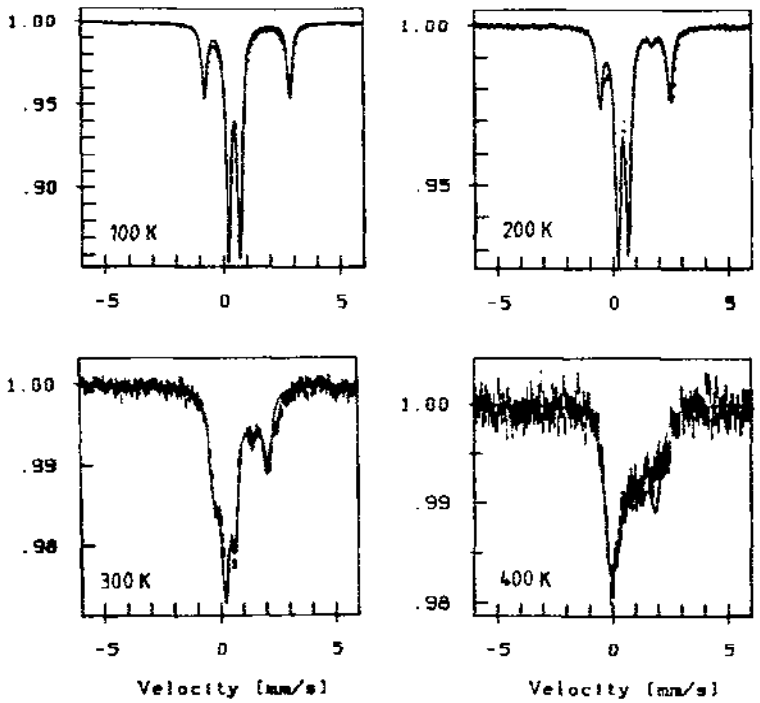

Fig. 10. Mössbauer spectra of $[Fe_{0.1}Zn_{0.9}tpchxn](ClO_4)_2$ at four different temperatures. The solid lines are simulations using a dynamic model [32].

of decay of the excited ^{57}Fe Mössbauer nuclei (1.4×10^7 s $^{-1}$). This has only recently been considered for iron(II) complexes, whereas several cases are known for iron(III) [31]. The present system was the first reported case [32]. In collaboration with Winkler [33] we have analysed the spectra within a generalized stochastic line profile theory and have obtained valuable information about the dynamics of the spin-state interconversion [32]. A careful study of the Mössbauer line profiles has revealed line broadening in several cases. Recently, Adler et al. have published an analysis of $[Fe(2\text{-pic})_3](PF_6)_2$ [35] and $[Fe(mepy)_3tren](PF_6)_2$ [34].

The analysis of the $[Fe(tpen)](ClO_4)_2$ case is complicated by the existence of at least two phases, one of which clearly shows line broadening [16]. The ratio between the high-spin and low-spin populations is known from susceptibility measurements. From the relaxation rates it is therefore possible to calculate the rate constant k_{15} for the low-spin to high-spin transformation and that for the reverse reaction (k_{51}). Plots of ln k_{15} or ln k_{51} values vs. the inverse temperature are linear in all cases, and the activation

parameters have been determined: $[Fe_{0.1}Zn_{0.9}tpchxn](ClO_4)_2$ $\Delta H_{15}^{\neq} = 13.1$ kJ mol^{-1}, $\Delta H_{51}^{\neq} = 6.7$ kJ mol^{-1} [18]; $[Fe(2\text{-pic})_3](PF_6)_2$ $\Delta H_{15}^{\neq} = 18.6$ kJ mol^{-1}, $\Delta H_{51}^{\neq} = 10.3$ kJ mol^{-1} [35], $[Fe(mepy)_3tren](PF_6)_2$, $\Delta H_{15}^{\neq} = 29.0$ kJ mol^{-1}, $\Delta H_{51}^{\neq} = 2.7$ kJ mol^{-1} [34]. Extrapolation from these values down to 40 K will in each case predict a very slow spin-state interconversion. The discovery of the so-called light-induced excited spin state trapping (LIESST) phenomenon [36] confirms that in some cases very slow kinetics are indeed observed.

(iii) Infrared spectroscopy

Spin change processes in solids can conveniently be followed by the temperature variation of the IR spectra.

Although the Fe–N stretch frequencies would be an obvious choice, they are often too weak and too difficult to assign. However, the CN stretch frequencies for coordinated NCS^-, $NCSe^-$ and $NCBH^-$ are good spin-state markers and have been used frequently [6,24,25].

As an example, there are the IR spectra in the CN stretch frequency region of *cis*-[Fe(bpen)$(NCS)_2$], shown in Fig. 11 at a temperature close to T_c and at a temperature above T_c.

The increase in the C–N stretching frequencies ν_{NC} of the NCS^- ligand in the spin cross-over system by 30 cm^{-1}, when the spin state changes from high spin to low spin, is typical for these kinds of systems [24,25]. We have suggested that the increase in ν_{NC} can be explained by an increase in the σ donation for the low-spin form compared with the high-spin form [24]. This

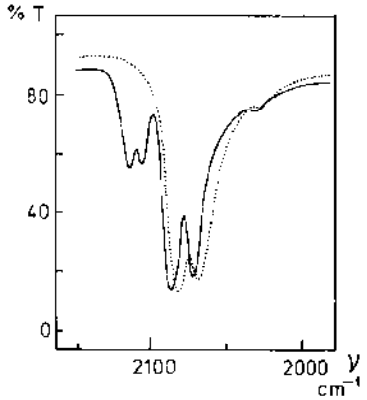

Fig. 11. The IR spectra of *cis*-[Fe(bpen)$(NCS)_2$] in the CN stretching region: — — —, recorded at 300 K; ———, recorded at 77 K [25].

will give the right shift because the lone pair at NCS is slightly antibonding. However, the suggestion by König and Madeja [28] that the shift is due to a stabilization of the low-spin form via π back-donation cannot be true, since it would have resulted in a shift in the opposite direction.

(iv) Crystal structures

In order to gain insight into which structural factors determine the spin state of a system, structure determination by X-ray diffraction on single crystals of spin-equilibria systems is an obvious technique. The structure of only a few systems has been determined up to now, and only in a few cases has it been possible to solve the structure above and below the critical temperature for the same system. From work on *mer*-$[Fe(2\text{-pic})_3]Cl_2 \cdot C_2H_5OH$, *mer*-$[Fe(2\text{-pic})_3]Cl_2 \cdot CH_3OH$ [38] and *mer*-$[Fe(2\text{-pic})_3]Br_2 \cdot C_2H_5OH$ [39] a common trend is that the Fe–N mean distances increase by 0.16 Å and 0.20 Å for the bond to the aliphatic and aromatic nitrogen atoms respectively on going from low spin to high spin. This result is in good agreement with the expected variation, if two electrons at iron(II) are shifted from non-bonding (t_{2g}) orbitals to antibonding (e_g) orbitals.

In a recent review by König [40] the structural changes accompanying spin-state transformations for a series of other systems in the literature were discussed.

In our group we have solved the structures of five systems, where the ligands in all cases are of the hexadentate polypodal picolyl type; $[Fe(tpchxn)](ClO_4)_2$ [18], $[Fe(tpen)](ClO_4)_2$, for which the structures of two different phases have been solved [16], $[Fe(tptcn)](ClO_4)_2$ [23] and $[Fe(tp[10]aneN_3)](ClO_4)_2$ [41]. Selected structural parameters for four of these systems are given in Table 3.

All the systems were solved at room temperature, where the systems are predominantly in the low-spin form. $[Fe(tpen)](ClO_4)_2$ (Fig. 2) has also been investigated at a high temperature, where the high-spin population is 25%. From these data it is possible to extrapolate to the high-spin geometry. Again a change in the Fe–N distances of about 0.19 Å is observed. The Fe–N(py) distances are expected to reflect a variation in the π-acceptor properties of the different systems. In the case of $[Fe(tptcn)](ClO_4)_2$ (Fig. 12) these distances are on average 0.01 Å shorter than for the other systems. This result is in agreement with the fact that this system is the only pure low-spin system in the series.

Owing to problems in growing large single crystals of the bis-isothiocyanato complexes, structural information on these types of systems is lacking. However, in one case, *cis*-$[Fe(bptn)(NCS)_2]$, we have carried out an extended X-ray absorption fine structure (EXAFS) study above and

TABLE 3

Selected distances (Å) and angles (degrees) in three different $[FeL]^{2+}$ [a]

Parameter [b]	L		
	tpen	tpchxn	tptcn
Distances			
Fe–N (aliphatic)	1.999(4)	2.01(1)	2.001(6)
Fe–N (picolyl) eq	1.988(6)	1.98(1)	1.979(6)
Fe–N (picolyl) ax	1.987(5)	1.99(2)	
N–C (aliphatic)	1.491(7)	1.60(2)	1.50(1)
N–C (picolyl) eq	1.488(7)	1.45(2)	1.479(9)
N–C (picolyl) ax	1.485(7)	1.52(1)	
N–C (imine chelate)	1.347(6)	1.39(1)	1.362(9)
C–C (aliphatic chelate)	1.514(8)	1.45(1)	1.52(1)
C–C (picolyl chelate)	1.475(8)	1.44(1)	1.50(1)
Angles			
N–Fe–N (aliphatic)	86.4(2)	89.8(1)	86.4(3)
N–Fe–N (picolyl) eq	111.5(2)	111.9(1)	94.8(2)
N–Fe–N (picolyl chelate) eq	81.0(2)	79.3(2)	83.1(2)
N–Fe–N (picolyl chelate) ax	84.2(2)	84.8(4)	
Fe–N–C (picolyl)	110.6(3)	107.6(1)	107.2(5)
Fe–N–C (aliphatic)	106.4(3)	105.0(1)	109.3(4)

[a] The uncertainties in the last figure are indicated in parentheses [16,18,23]. [b] eq, equilibrium; ax, axial.

below the transition temperature (170 K). The fitting of the data suggests that four of the Fe–N distances change by 0.20 Å, whereas the remaining two distances change only by 0.05 Å. This result indicates that the change in bond order for these particular bonds is very low. We suggest that the two unchanged distances represent the Fe–NCS bonds [29].

Structural correlations

An important parameter in the discussion of the geometry of pseudooctahedral systems is the twist angle ϕ between the two opposite trigonal faces. Figure 13 shows how this angle is defined for a facial isomer of an $Fepy_3N_3$ complex.

A series of structure determinations on tris dithiocarbamate iron(III) complexes show that small values of ϕ are correlated with high values of [HS]/[LS] [42]. Such a tendency can be predicted with the help of force-field calculations based on classic considerations. Defining the normalized bite b as the distance between the donor atoms in a chelate, BITE, divided by the metal–ligand distance, Kepert [42] has suggested a correlation between ϕ and b.

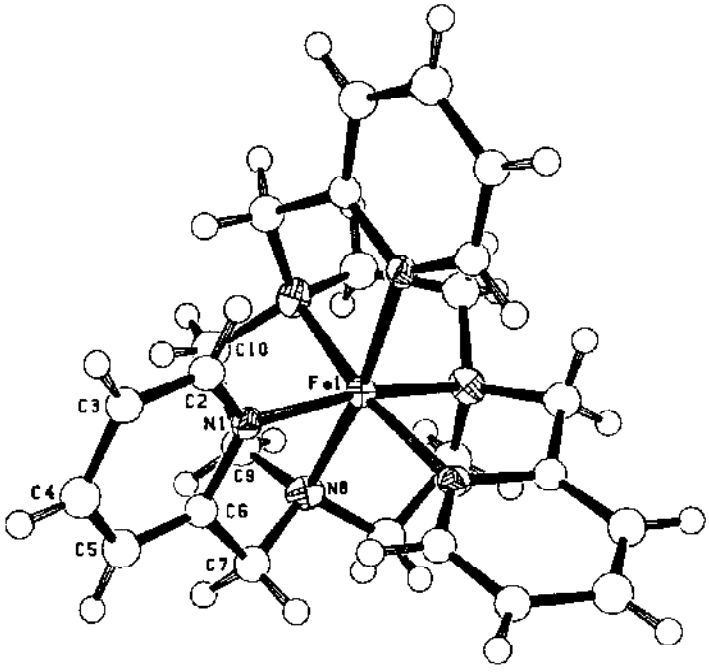

Fig. 12. ORTEP drawing of the molecular structure of one of the three crystallographically inequivalent cations in $[Fe(tptcn)](ClO_4)_2$ [23].

For $b = \sqrt{2}$ the potential surface has a pronounced minimum at $\phi = 60°$, corresponding to the octahedron. However, if b decreases, the minimum will be shifted to lower ϕ values, corresponding to an octahedron, which is trigonally twisted around the threefold axis.

In the case of relatively stiff chelating ligands such as dithiocarbamates and diimines, the BITE values are more or less fixed, so that if the metal

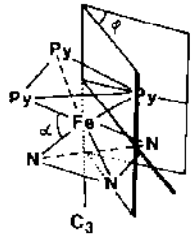

Fig. 13. Definition of two structural parameters; the twist angle ϕ and the chelate bite angle α [23].

TABLE 4

Structural parameters

Complex	BITE (Å)	TOP (Å)	ϕ (deg)	α (deg)
Ideal octahedron [a]	2.828	2.828	60	90
Trigonal prism [a]	2.619	2.619	0	81.8
fac-[Fe(2-pic)$_3$]Cl$_2$ [b]	2.638	2.950	53.7	82.3
mer-[Fe(2-pic)$_3$]Cl$_2$ [b]	2.715	3.301	41.1	76.9
[Fe(tp[10]aneN$_3$)](ClO$_4$)$_2$ [c]	2.621	2.881		82.4
[Fe(tptcn)](ClO$_4$)$_2$ [d]	2.640	2.724	48.9	83.1
[Mn(tptcn)](ClO$_4$)$_2$ [c]	2.750	2.872	19.6	75.7
[Ni(tptcn)](ClO$_4$)$_2$ [e]	2.693	2.805	46.8	81.1
[Fe(tpchxn)](ClO$_4$)$_2$ [f]	2.857	2.753	55.1	89.8
[Fe(tpen)](ClO$_4$)$_2$ [g]	2.734	2.771	55.0	86.4
[Fe(HBpz)$_2$] [h]	2.749	2.831	59.0	91.7
[Fe(HBme$_2$pz)$_2$] [h]	2.993	3.148	56.5	92.9

[a] Assuming a metal–ligand distance of 2.00 Å. [b] Ref. 44. [c] Ref. 41. [d] Ref. 23. [e] Ref. 45. [f] Ref. 18. [g] Ref. 23. [h] Ref. 46.

ligand distance is increased, the b value will decrease. Therefore we shall expect to observe small values of ϕ for the HS complexes, compared with those for the corresponding LS complexes. This tendency is further amplified in d^6 systems, because the LS d^6 electronic configuration ($^1A_1$) has exactly the highest possible octahedral preference energy. Recently Gladstone et al. [43] have discussed the coordination geometry of hexadentate tripod ligands. They have introduced one extra parameter, TOP, which is the distance between the donor atoms along an edge not bridged by a chelate ring.

In Table 4, BITE and TOP parameters are compared for a series of related complexes. Some of the systems in the table do not have true threefold axes, however, and for these systems pseudothreefold axes can be defined. According to Gladstone et al. [43] BITE and TOP are correlated for constant metal–ligand distances; therefore systems with the same ϕ should lie on a straight line in a BITE, TOP diagram. The data in Table 4 are not suitable for testing this hypothesis because the three metal–ligand distances vary quite considerably throughout the series. Only the $[Mn(tptcn)]^{2+}$ system has a geometry which is nearly trigonal prismatic. As HS manganese(II) has no ligand field stabilization, the geometry of this complex will probably reflect the strain-free geometry. The ϕ found for $[Fe(tptcn)]^{2+}$, 48.9°, probably reflects a compromise between steric and electronic effects.

D. CHARACTERIZATION OF SPIN EQUILIBRIA IN SOLUTION

A system which is a spin cross-over system in the solid will in many cases also show a spin equilibrium in solution. However, only a few systems have been fully characterized in solution.

In order to have a true spin equilibrium in solution the system must be reasonably inert with respect to ligand dissociation. This requirement is very well fulfilled for systems based on hexadentate ligands, as these systems have stability constants of the order of 10^{25}. Furthermore, the flexibilities are often so restricted (by the fusion of many chelate rings) that the structures found for the molecular cation in the solid represent the geometry of the ion in solution very well.

(i) Electronic spectra

The electronic spectra of a series of octahedral iron(II) complexes with nitrogen donor atoms are given in Table 5. Many of these complexes are spin-equilibria systems in aqueous solution around room temperature. As a

TABLE 5

Electronic spectra of iron(II) complexes in water

Complex	MLCT		$^1T_1 \leftarrow {}^1A_1$		$^5E \leftarrow {}^5T_2$	
	λ (nm)	ϵ	λ (nm)	ϵ	λ (nm)	ϵ
$[Fe(2\text{-pic})_3]^{2+}$ [a]	440	4200	581		730	
$[Fe(tptan)]^{2+}$ [g]	369	1130				
$[Fe(tpted)]^{2+}$ [g]	362	1120				
$[Fe(tpten)]^{2+}$ [g]	434	12230				
$[Fe(dpa)_2]^{2}$ [b]	433					
$[Fe(blbpen)]^{2+}$ [h]	359	1640			839	9
$[Fe(hpen)]^{2+}$ [h]	370	1600			790	
$[Fe(tpbn)]^{2+}$ [i]	354	1623				
$[Fe(tpen)]^{2+}$ [h]	414	7810	545	100		
$[Fe(tpchxn)]^{2+}$ [h]	419	8700	544	100		
$[Fe(tppn)]^{2+}$ [h]	425	10670	545	100		
$[Fe(tpmbn)]^{2-}$ [i]	421	13600	550	100		
$[Fe(tptn)]^{2+}$ [h]	425	11310	550	100		
$[Fe(iox)_6][ClO_4)_2$ [c]	375		549		847	
$[Fe(pybenH)_3]^{2+}$ [d]	496	1680				
$[Fe(HBpz)_2]$ [e]	337		535			
$[Fe(py)_3tren]^{2+}$ [f]	360,510,560					

[a] Ref. 47. [b] Ref. 12. [c] Ref. 48. [d] Acetonitrile [18]. [e] Ref. 49. [f] Ref. 50. [g] Ref. 23. [h] Ref. 13. [i] Ref. 18.

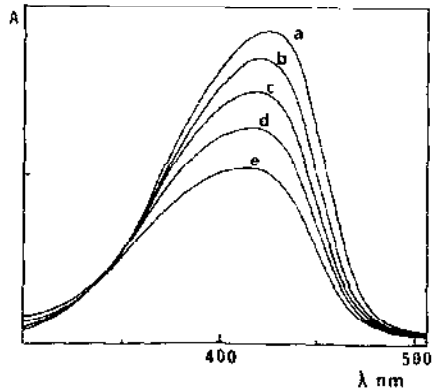

Fig. 14. Temperature variation of the electronic spectrum of $[Fe(tpchxn)](ClO_4)_2$ in water: (a) 12.2, (b) 24.4, (c) 39.4, (d) 53.5, (e) 68.6 °C [17].

rule these systems show a dramatic thermochromism, and the spectral variations can be used in the characterization of the spin equilibrium. However, it will seldom be possible to cover the whole temperature range of the complete low-spin to high-spin transition.

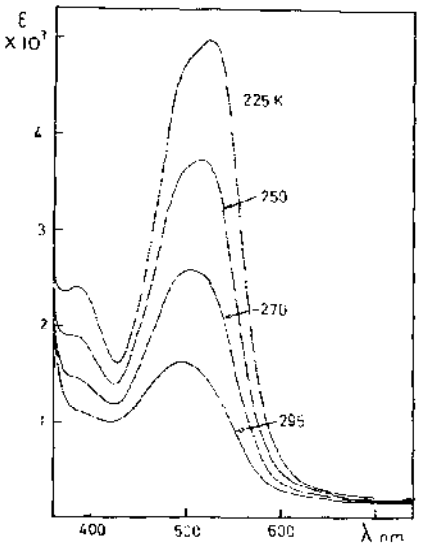

Fig. 15. Temperature variation of the electronic spectrum of $[Fe(pybenH)_3](ClO_4)_2$ in acetonitrile [18].

Figures 14 and 15 show typical examples of spectral changes in the metal-to-ligand charge transfer (MLCT) region of the low-spin component in spin-equilibria systems. Even with a temperature variation of 70 K the pure low-spin and high-spin spectra can only be obtained by extrapolation [17].

When the spectra of the pure components are known, the equilibrium constant [HS]/[LS] can be calculated for each temperature. From such data $\Delta H°$, $\Delta S°$, and T_c can be evaluated. However, data obtained in this way are not as reliable as those obtained from a direct determination of the susceptibility on the solutions (see later).

From the electronic spectra an estimate of the ligand field parameter has been obtained. These data are useful in a discussion of the correlation between different systems. It is normally fairly easy to observe the $^5E \leftarrow {}^5T_2$ transition around 800 nm for the high-spin components. However, for iron(II) complexes of imine ligands the $^1T_1 \leftarrow {}^1A_1$ and $^1T_2 \leftarrow {}^1A_1$ transitions of the low-spin forms are in general masked by intense MLCT transitions at about 420 nm [13].

For the systems in Table 5 where the position of the $^1T_1 \leftarrow {}^1A_1$ transition is listed it has been possible to obtain that information from a Gauss curve analysis of the low-energy part of the charge transfer band.

In the case of [Fe(*R*-tppn)]$(ClO_4)_2$ and [Fe(*R*,*R*-tpchxn)]$(ClO_4)_2$ the ligand field transitions were also observed in the circular dichroism (CD) spectra at 544 nm and 545 nm respectively. These values are reliable as the ligand field CD bands in this part of the spectrum are disturbed only very little by the charge transfer bands [13]. For none of the systems in Table 5 has it been possible to observe the $^1T_2 \leftarrow {}^1A_1$ transition, so an exact calculation of the ligand field strenth Δ_{ls} was not possible.

Recently, two cases have been reported where both the ligand field bands were observed in spin-equilibria systems [36,51]. From these data, Δ_{ls} values of 20030 cm^{-1} and 18610 cm^{-1} respectively are obtained.

For the isoelectronic cobalt(III) systems the charge transfer bands are blue shifted so much that the ligand field bands are clearly seen. This fact makes it possible to correlate Δ for cobalt(III) and iron(II) with the prospect of predicting the critical Δ value for other systems.

Table 6 shows the ligand field transitions and the calculated parameters for a series of cobalt(III) complexes, corresponding to the iron(II) complexes in Table 5.

Using the ratio $\Delta(Co(III))/\Delta_{ls}(Fe(II)) = 1.20$, a critical value for Δ_{ls} of 18450 cm^{-1} is estimated, close to the value found from the cage system [51] and the value suggested by Chum et al. [47].

The $^5E \leftarrow {}^5T_{2g}$ transition has only rarely been observed for spin-equilibria systems, mainly because of the very weak intensity of this transition. The

TABLE 6

Electronic spectra of cobalt(III) complexes in water

Complex	$^1T_2$		$^1T_1$		Δ (10^3 cm^{-1})	B (10^3 cm^{-1})
	λ (nm)	ϵ	λ (nm)	ϵ		
mer-$[Co(2\text{-pea})_3]^{3+}$ [a]	342	sh [e]	475	193	22.69	0.60
fac-$[Co(2\text{-pea})_3]^{3+}$ [a]	338	sh	466	150	23.09	0.60
fac-$[Co(2\text{-pic})_3]^{3+}$ [a]	336	sh	462	130	23.28	0.59
$[Co(tptan)]^{3+}$ [b]	340	sh	482	300	22.47	0.65
$[Co(tptcd)]^{3+}$ [b]	340	sh	496	300	21.99	0.71
$[Co(tpten)]^{3+}$ [b]	347	255	473	292	22.69	0.56
$[Co(blbpen)]^{3+}$ [d]	355	400	513	252	21.21	0.66
$[Co(ltpen)]^{3+}$ [c]	341	400	483	303	22.42	0.65
$[Co(tpen)]^{3+}$ [c]	328	400	468	313	23.18	0.69
$[Co(tpchxn)]^{3+}$ [d]	331	400	474	300	22.91	0.69
$[Co(tppn)]^{3+}$ [c]	330	400	470	314	23.07	0.68
$[Co(tpmbn)]^{3+}$ [d]	342	350	475	267	22.69	0.60
$[Co(tptn)]^{3+}$ [c]	328	sh	465	111	23.29	0.67

[a] Ref. 11. [b] Ref. 23. [c] Ref. 13. [d] Ref. 18. [e] sh, shoulder.

bands are usually split due to the Jahn–Teller instability of the ^5E state. The best estimate of Δ_{hs} will be the midpoint between the two split components.

The value found by Hauser et al. [36] for single crystals of $[Fe(ptz)_6](BF_4)_2$, $\Delta_{hs} = 12500$ cm^{-1}, is in good agreement with the values found for the systems in Table 5. However, the Δ_{hs} value of 13700 cm^{-1} [47] found for $[Fe(2\text{-pic})_3]^{2+}$ is surprisingly high.

As the crystal field model predicts that Δ is proportional to the inverse fifth power of the metal–ligand distance, we shall expect that Δ_{hs}/Δ_{ls} should be $(R_{ls}/R_{hs})^5 = (2.00/2.17)^5 = 0.65$. The actual value of 0.66 is in excellent agreement with this prediction.

The large difference between the critical ligand field strengths Δ_{hs} and Δ_{ls} has the consequence that the "crossing point" in the common energy diagrams is not just a point but a whole region of non-accessible Δ values, ranging from Δ_{hs} to Δ_{ls} (see Fig. 16). No complex with a Δ value within that region can exist as it will be energetically more favourable for it either to contract and form a low-spin complex or to expand and form a high-spin complex. Orgel [2] was the first to realize this point.

In Fig. 16, strict octahedral geometry has been assumed. Most spin cross-over complexes have a symmetry lower than octahedral. If the ligand field deviates strongly from octahedral symmetry an intermediate spin state (triplet) can become the ground state.

The condition for spin equilibrium is that the Δ value is approximately outweighed by the spin-pairing energies P. Since the spin-pairing energies

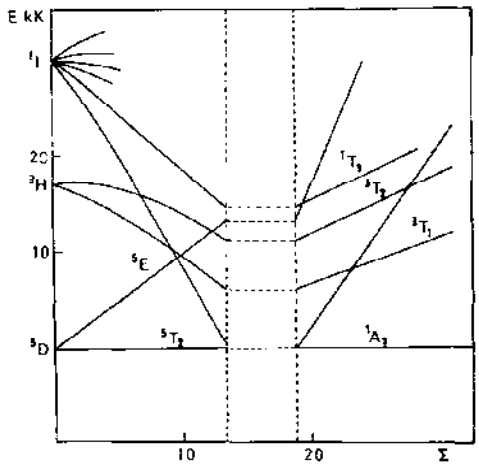

Fig. 16. Modified Tanabe–Sugano diagram for d^6.

are different for the two spin states, it has become a practice to refer to the mean spin-pairing energy $\bar{P}$ and the spin-equilibrium condition is then expressed as $\bar{P} = \Delta$.

P is usually expressed in units of the interelectronic repulsion parameter Racah B. In the crystal field model, B is taken from the free gaseous ion. In a more realistic ligand field description, B should, however, be more or less reduced according to the covalency of the metal–ligand bonds (the nephelauxetic effect). As a rule soft ligands such as carbon, sulphur, phosphorus and arsenic donors will favour low spin. Harder ligands such as nitrogen donors can in some cases also lead to unusually low B values.

$[Fe(tptcn)]^{2+}$ should according to the Δ value be a cross-over system, but it is actually a pure low-spin complex. A closer examination of the electronic spectrum of the corresponding cobalt(III) complex [23] reveals a marked reduction in B compared with that for other similar complexes. Therefore in this case the resulting spin state is determined by the high nephelauxetic effect of the metal complex. We suggest that the increased covalency in this case is due to the macrocyclic part of the ligand.

Another example is $[Fe(dppen)_2]Cl_2$ which is a spin-equilibrium system [52]. However, Δ_{hs} and Δ_{ls} are only about 80% of the values required for a spin-equilibrium system. In this case the spin-equilibrium condition has been achieved by the unusually high nephelauxetic effect of the phosphorus donor atoms.

The dimensionless parameter $\Sigma = \Delta/B$ has been suggested as a measure of relative ligand field strength. Unfortunately, it has been possible only in a

few cases to determine B for an iron(II) spin-equilibrium system. In Fig. 16 a B value of 925 cm^{-1} has been chosen, which gives a critical range of $13.3 < \Sigma < 20.0$.

A B value of about 900 cm^{-1} might be acceptable for the high-spin form, but it is far too high for the low-spin form. Very recently the electronic spectrum for a spin-equilibrium system showing both the low-spin ligand field bands has been reported [51]. On the basis of these data a B(ls) value of 660 cm^{-1} has been calculated, so that the critical Σ value can be as high as 28. Thus $\Sigma(ls)/\Sigma(hs) \approx 2$.

The difference in ligand field stabilization of two spin states is crucial in determining which state will be the ground state. As a result it is the magnitude of Δ_{ls} in comparison with $\bar{P}$ which is most important because

$$\bar{P} = \frac{2.4\Delta_{ls} - 0.4\Delta_{hs}}{2}$$

The electron degeneracy of the high-spin state is 15 times that of the low-spin state. As a consequence the high-spin state is favoured by a free energy contribution of about 550 cm^{-1} at room temperature, due to the entropy term. Therefore the best opportunity for the observation of spin equilibrium around room temperature ($K_{eq} \approx 1$) will be achieved in the case where $\bar{P} - \Delta_{ls} \approx 550$ cm^{-1}. From the relation above, a typical value of 19750 ± 600 cm^{-1} for $\bar{P}$ is obtained.

$\bar{P} - \Delta_{ls}$ will typically be of the order of magnitude of 1000 cm^{-1}, corresponding to a situation in which the true ground state is low spin, while several percent of the high-spin form is populated at room temperature.

As mentioned earlier, the ligand field bands of spin-equilibria systems are rarely observed. Therefore correlations between ligand field parameters for different ligands can be based on the spectra of corresponding cobalt(III) and nickel(II) complexes only.

Cobalt(III) complexes are generally low spin; therefore Δ values determined from these are expected to correlate with Δ_{ls} for the corresponding iron(II) complexes.

Spectral data for a series of related cobalt(III) complexes are listed in Table 6. As the two first spin-allowed ligand field transitions can be observed in these complexes, it has been possible to calculate both Δ and B. The Σ values vary from 30 to 41, which is about twice the value found for the corresponding iron(II) systems. In an analogous way the spectra of the nickel(II) complexes can be used to judge the Δ_{hs} values. All the nickel(II) complexes investigated show spectral features typical for near-octahedral geometry. Table 7 lists the positions of the two first spin-allowed ligand field transitions as well as the Δ and B values for a series of analogous nickel(II) complexes.

TABLE 7

Electronic spectra of nickel(II) complexes in water

Complex	$^3T_2$		$^3T_1$		Δ (10^3 cm^{-1})	B (10^3 cm^{-1})
	λ (nm)	ε	λ (nm)	ε		
$[Ni(2\text{-pic})_3]^{2+}$ [a]	856	16	527	25	11.68	0.61
$[Ni(2\text{-pea})_3]^{2+}$ [a]	859	18	528	30	11.64	0.61
$[Ni(tptcd)]^{2+}$ [b]	930		554	17	10.8 [c]	0.6
$[Ni(tptan)]^{2+}$ [b]	928		555	14	10.8 [c]	0.6
$[Ni(tptcn)]^{2+}$ [b]	818	33	512	22	12.35 [d]	0.58
$[Ni(blbpen)]^{2+}$ [e]	963	27	551	11	10.42	0.65
$[Ni(ltpen)]^{2+}$ [e]	929	25	527	14	10.81	0.69
$[Ni(tpbn)]^{2+}$ [f]	878	11	529	17	11.4 [c]	0.6
$[Ni(tpen)]^{2+}$ [e]	822	23	517	14	11.27 [d]	0.68
$[Ni(tpchxn)]^{2+}$ [e]	816	29	518	19	11.33 [d]	0.67
$[Ni(tppn)]^{2+}$ [e]	822	26	517	17	11.36 [d]	0.67
$[Ni(tpmbn)]^{2+}$ [f]	815	24	516	17	11.83 [d]	0.63
$[Ni(tptn)]^{2+}$ [e]	805	11	510	11	12.25	0.64

[a] Ref. 11. [b] Ref. 23. [c] Estimated value. [d] Corrected for the interaction with the singlet state. [e] Ref. 13. [f] Ref. 18.

Using the ratio $\Delta_{hs}(Fe(II))/\Delta\ Ni(II) = 1.05 \pm 0.3$, suggested by Nelson and Rodgers [12], it is expected that if a nickel(II) complex has a value in the range 11 300–11 900 cm^{-1} then the corresponding iron(II) complex is also expected to be a spin-equilibrium complex. This is remarkably well fulfilled in the present series. As B is normally a little less for a nickel(II) complex than for the corresponding iron(II) complex, the Σ values for iron(II) and nickel(II) complexes will be nearly identical.

(ii) Magnetic susceptibility in solution

Magnetic susceptibility measurements in solution are still relatively rare, probably because the main interests in the field have been devoted to solid state effects.

The preferred technique has been Evan's method, although the accuracy obtained by this method is not as high as the accuracy achieved by using the Faraday method [17]. As a general trend, spin-equilibria systems in solution are gradual. This is of course expected as no cooperative effects can act in a dilute solution.

Figure 17 shows the variation in μ_{eff} with temperature for a series of 2-methoxyethanol water solutions of iron(II) complexes of tpen-type ligands. All these systems have critical temperatures T_c close to or above room temperature [17]. The temperature range required for a full low-spin to

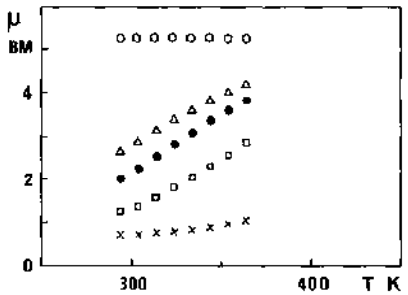

Fig. 17. Temperature variation of the magnetic moment μ_{eff} for a series of spin-equilibria systems in water–2-methoxyethanol (1:1 v/v) solutions [17]: △, $[Fe(tpchxn)](ClO_4)_2$; ●, $[Fe(tpen)](ClO_4)_2$; ○, $[Fe(blbpen)](ClO_4)_2$; □, $[Fe(tppn)](ClO_4)_2$; ×, $[Fe(tptn)](ClO_4)_2$.

high-spin conversion (around 150 K) is unfortunately not accessible with common solvents.

Thermodynamic parameters for the ${}^1A_{1g} \rightleftarrows {}^5T_{2g}$ equilibrium can in most cases be evaluated from $\ln K_{eq}$ vs. $1/T$ plots.

Table 8 lists the thermodynamic parameters found for a series of spin-equilibria systems in different solvents. Most of these systems are also

TABLE 8

Thermodynamic parameters for spin-equilibria systems in solution

Complex	Solvent	ΔH^0 (kJ mol^{-1})	ΔS^0 (J K^{-1} mol^{-1})	T_c (K)
$[Fe(2\text{-pic})_3](ClO_4)_2$	CH_3OH-H_2O	18.0	52.3	344 [a]
$[Fe(2\text{-pic})_3](ClO_4)_2$	CH_3CN-H_2O	21.3	72.0	297 [a]
$[Fe(2\text{-pic})_3]Cl_2$	CH_3CN-H_2O	24.7	87.9	281 [a]
$[Fe(tpen)](ClO_4)_2$	DMF	26.4	72.8	363 [b]
$[Fe(tpen)](ClO_4)_2$	2-Methoxyethanol–H_2O	23.9	67.0	356 [b]
$[Fe(tpen)]I_2$	2-Methoxyethanol–H_2O	29.6	74.5	398 [b]
$[Fe(tpchxn)](ClO_4)_2$	DMF	23.6	64.9	365 [b]
$[Fe(tpchxn)](ClO_4)_2$	CH_3CN	24.4	75.3	340 [b]
$[Fe(tppn)](ClO_4)_2$	DMF	25.4	70.7	360 [b]
$[Fe(tppn)](ClO_4)_2$	CH_3CN	29.8	87.9	338 [b]
$[Fe(tppn)](ClO_4)_2$	2-Methoxyethanol–H_2O	30.2	77.0	392 [b]
$[Fe(tpmbn)](ClO_4)_2$	DMF	30.0	74.5	402 [b]
$[Fe(tptn)](ClO_4)_2$	DMF	45.1	49.0	496 [b]
$[Fe(pyim)_3](BPh_4)_2$	$(CH_3)_2CO$	15	53	294 [c]
$[Fe(pyben)_3](BPh_4)_2$	$(CH_3)_2CO$	20	78	253 [c]
$[Fe(pyben)_3](BPh_4)_2$	CH_3CN-CH_3OH	21	92	232 [c]
$[Fe(HBpz)_2]$	$(CH_3)_2CO$	16.1	47.7	338 [d]
$[Fe(mepy)_2pytren](PF_6)_2$	$(CH_3)_2CO$	15	50	300 [e]

[a] Ref. 47. [b] Ref. 17. [c] Ref. 53. [d] Ref. 49. [e] Ref. 50.

spin-equilibria systems in the solid state even though the parameters found in the solid differ considerably from the solution values. In the case of $[Fe(pen)](ClO_4)_2$ the following values have been found in the solid; $\Delta H^\circ = 25.6$ kJ mol^{-1}, $\Delta S = 67.4$ J K^{-1} mol^{-1} and $T_c = 380$ K. The trend is that T_c is lowest for the solution, probably a reflection that the lattice energies contribute more to the ligand field energy than do the solvation energies.

The variation in the thermodynamic parameters from one solvent to another is relatively modest, although it seems to follow the expected pattern that polar systems favour low spin. Systems such as $[Fe(2\text{-pic})_3]^{2+}$, with groups that can establish hydrogen bonds to polar solvents, show rather large changes in T_c, depending on the solvent used.

Changes in the anion can result in a change of T_c both in the solid state and in solution. This effect has a natural explanation in the case of the solid state. However, it is less obvious why there should be any effect in solution. Nevertheless, changing perchlorate for iodide in the $[Fe(tpen)]X_2$ systems gives a T_c which is 35 K higher [17]. We suggest that the effect is due to changes in the degree of ion pairing. The importance of ion pairing in this type of system has very recently been confirmed by Conti et al. [54].

E. DYNAMIC ASPECTS OF SPIN CHANGE REACTIONS

The last few decades have witnessed great activity in the study of intermolecular and intramolecular electron transfer processes in transition metal complexes. The interchange between high-spin and low-spin states of metal ions may represent the simplest intramolecular electron transfer process, and an understanding of the detailed mechanism for the spin interconversion process is therefore highly desirable. Recently, Bacci [55(a)] and Beattie [55(b)] have reviewed the static and the dynamic effects in spin-equilibria systems.

From a chemical point of view the interest in spin-state dynamics of iron(II) derives from the question of how it may influence the kinetics of reactions such as electron transfer, hydrolysis and racemization.

In the following part we shall discuss which electronic and geometric factors are the most important in determining the rates of spin-state changes, and we shall try to interpret the observations within a theoretical framework such as the model of radiationless multiphonon processes by Buhks et al. [56] and a conventional description of the activation energy as an inner-sphere reorganization energy [57].

(i) Experimental techniques

The applied techniques are dictated by the typical range of rate constants, 10^6–10^9 s^{-1}, in solution at room temperature. This fact limits the choice of

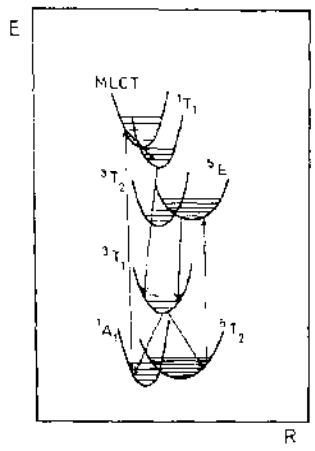

Fig. 18. Cross-section in the potential surfaces of the ground state and excited states of an iron(II) spin-equilibrium system. The arrows indicate how a photochemical perturbation of the equilibrium can be achieved.

techniques to the relaxation methods. Beattie and coworkers [55(b),58,59] have investigated a few iron(II) and iron(III) systems by an ultrasonic relaxation technique, covering rates up to 10^8 s^{-1}. Wilson and coworkers [60–63] pioneered the use of laser Raman temperature-jump measurement on a series of iron(II) and iron(III) systems.

Recently, McGarvey et al. [64,65] have demonstrated the feasibility of variable-temperature rate determination by a laser-induced photochemical perturbation technique, where the laser frequencies are chosen to overlap with the charge transfer absorption of the LS complexes. The charge transfer bands of the high-spin forms are as a rule found in the UV region of the spectrum; therefore it is easy to achieve a selective excitation of the low-spin molecules in a spin-equilibrium mixture. The only prerequisite required for the use of the technique is that the lifetime of the optically pumped excited spin state is long enough to be detected.

In Fig. 18 the potential energy surfaces for the states derived from an iron(II) spin-equilibrium system are shown, and a mechanism for the photochemical population of the $^5T_2$ state is suggested. The MLCT states initially populated are very short lived and can rapidly decay to the nearby excited ligand field states $^1T_1$ and $^1T_2$. These states are also short lived and can rapidly decay back into the $^1A_1$ ground state. However, an alternative decay path, via the $^3T_1$ and $^3T_2$ ligand field states, can lead to a population of the $^5T_2$ state. There is no radiative relaxation between the $^5T_2$ and the $^1A_1$ states. Therefore any relaxation between these states is expected to occur via an

adiabatic thermal excited path. Thus the ground state recovery rate is a direct measure of the relaxation of the spin-equilibrium mixture, as this is the rate-determining step. A similar scheme has been suggested as an explanation of the LIESST phenomenon [36].

The experimental convenience of this technique has greatly widened the range of conditions which can be investigated. Thus McGarvey et al. [64,65] have included pressure studies in a variety of solvents, and Hendrickson and coworkers [54,66] have greatly extended the accessible temperature range by using polymer film solution.

(ii) Discussion

Table 9 lists the activation parameters found for a series of iron(II) spin-equilibria systems in different solvents. The observed rate constants around room temperature are all in the range 10^6–10^8 s^{-1}. We wish to stress that although these rate constants are large by chemical standards, they are still many orders of magnitude smaller than the rate constants for spin-allowed transitions. Actually, the spin-state transition probability calculated for an octahedral iron(II) system, calculated to first order, is zero.

Early determinations of activation parameters are rather inaccurate, and often the thermodynamic parameters were not well determined. Sutin and coworkers [57] and Beattie [55(b)] analysed these data in terms of the absolute rate theory. Assuming that the transition state resembles the ^5T state ($\Delta H_{51}^{*} \approx 0$), barrier transmission coefficients κ in the range 10^{-2} 10^{-3} were estimated. Such small values for κ indicate a non-adiabatic character of the reaction. Newer and more accurate data, however, show that both ΔH_{15}^{*} and ΔH_{51}^{*} are of the same order of magnitude [17,64,65]. A free energy plot ($\ln K$ vs. $\ln k$) for the forward (1–5) and backward (5–1) reactions define a fairly good line with a slope of 0.5 (Fig. 19). This suggests a common mechanism for which the transition state has a geometry intermediate between that of the ^1A spin isomer and that of the ^5T spin isomer.

Dose et al. [57] conclude from their data that non-electronic factors are significant in determining the rates of spin-state changes. In spite of the fact that systems with bidentate, tridentate and hexadentate ligands are represented in the list in Table 9, no dramatic changes in rates from steric effects are apparent from the data. Only in a single case ([Fe(tpchxn)]$(ClO_4)_2$ in dimethylformamide (DMF)) has a significant deviation from the general trend been observed.

In all models attempting to predict spin-change rates, the change in the metal–ligand distances, Δr_0, between HS and LS molecules is a crucial parameter. This is in line with the assumption that the main contribution to the activation process is an inner-sphere reorganization energy.

TABLE 9

Activation parameters for iron(II) spin-equilibria systems in various solvents

Complex	Solvent	k_{obs} 295 K (s^{-1})	$\Delta H°$ (kJ mol^{-1})	$\Delta S°$ (J mol^{-1} K^{-1})	$\Delta H^{\neq}_{15}$ (kJ mol^{-1})	$\Delta H^{\neq}_{51}$ (kJ mol^{-1})	ΔV^{0} (cm^3 mol^{-1})	$\Delta V^{\neq}_{15}$ (cm^3 mol^{-1})	$\Delta V^{\neq}_{51}$ (cm^3 mol^{-1})	$\Delta S^{\neq}_{15}$ (J mol^{-1} k^{-1})
$[Fe(HB(Pz)_3)_2]$ [a]	THF	3.0×10^7	21.0	57.0	23.6	7.6				−37.2
$[Fe(paptH)_2]^{2+}$ [b]	H_2O	2.4×10^7	16.4	62.0	31.9	15.6				0.4
$[Fe(pyimH)_3]^{2+}$ [c]	CH_3OH CH_3CN (20%)	2×10^7	15.5	52.7	26.1	10.6	5.3	0	−5.3	−23.0
$[Fe(pyimH)_3]^{2+}$ [c]	CH_3COCH_3	1.5×10^7	15.9	48.5	30.8	14.9	10.3	4.9	−5.4	−9.0
$[Fe(pyimH)_3]^{2+}$ [c]	CH_3CN						14.3	8.9	−5.4	44.0
$[Fe(pyben\ H)_3]^{2+}$ [c]	CH_3OH CH_3CN (20%)	2.6×10^7	21.3	92.0	29.1	7.8	4.3	0.2	−4.1	−9.0
$[Fe(pyben\ H)_3]^{2+}$ [c]	CH_3COCH_3	3.4×10^7	19.7	78.0	33.2	13.5	9.6	4.7	−4.9	10.0
$[Fe(pyben\ H)_3]^{2+}$ [c]	CH_3CN						12.4	5.9	−6.4	21.0
$[Fe(ppa)_2]^{2+}$ [d]	H_2O	9.7×10^6	21.6	44.0	34.1	12.5				−25.0
$[Fe(ppa)_2]^{2+}$ [d]	CH_3COCH_3	5.6×10^6	20.0	52	33.0	13.0				−21.0
$[Fe(L(VII))_2]^{2+}$ [d]	CH_3COCH_3	9.1×10^6	23.8	94.2	32.6	8.8	12.3	3.9	−8.4	
$[Fe(tpchxn)]^{2+}$ [e]	DMF	7.2×10^6	21.1	62.3	56.0	29.7	15.5	23.9	11.3	49.0
$[Fe(tpen)]^{2+}$ [f]	CH_3OH–H_2O	3.3×10^7	18.3	48.1	30.4	14.3				−12.7

[a] Ref. 58. [b] Ref. 59. [c] Ref. 65. [d] Ref. 70. [e] Ref. 17. [f] Ref. 16.

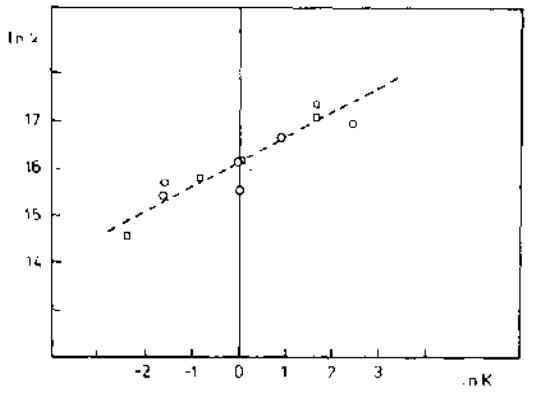

Fig. 19. Free-energy correlation for a series of spin-change reactions: ○, for k_{15}; □, for k_{51} [18].

Dose et al. [57] claim that their data show a correlation between the magnitude of Δr_0 and the observed rate constants. A close resemblance of HS and LS forms (small Δr_0), favours fast interconversion. Unfortunately the Δr_0 values for the systems in Table 9 are only known indirectly, and they do not vary much, so a quantitative correlation cannot be established.

The high pressure behaviour of spin cross-over systems is often complicated and unpredictable, whereas solution studies in the pressure range 0.1–125 MPa are in accordance with the expectation of a positive partial molar volume ΔV_{15}^0 for the LS → HS process. Values in the range 4–22 cm^3 mol^{-1} have been reported. Considering the typical Δr_0 value of 0.2 Å found from X-ray diffraction or EXAFS studies on the solids, the observed values of ΔV_{15}^0 are too small.

Assuming that the size of the ligands remains constant, a ΔV_{15}^0 value of about 25 cm^3 mol^{-1} is expected. The conclusion is that in most cases the increase in the size of the central ion is partly compensated by a contraction either in the ligand sphere or in the solvent sphere.

Figure 20 shows the volume of activation as a function of the donor number DN of the solvent [67] for two related systems [65]. Both ΔV_{15}^0 and $\Delta V_{15}^{\neq}$ are positive and strongly solvent dependent, whereas $\Delta V_{51}^{\neq}$ is negative and nearly independent of the solvent. As the observed value $\Delta V_{obs}^{\neq}$ in general consists of an intrinsic contribution $\Delta V_{int}^{\neq}$ and a solvent contribution $\Delta V_{solv}^{\neq}$, the solvent independence of $\Delta V_{51}^{\neq}$ suggests that the main contribution to this parameter arises from the Fe–N bond contraction in the $^5T \rightarrow {}^1A$ activation step.

Both ΔV^0 and $\Delta V_{15}^{\neq}$ are correlated with the nucleophilic properties of the solvent, becoming less positive with decreasing solvent donor number. The

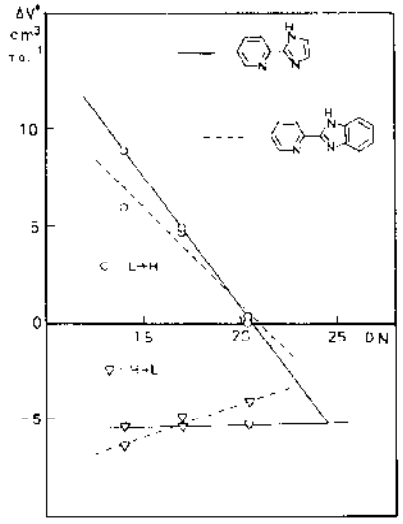

Fig. 20. Variation in the volume of activation as a function of the donor number of the solvent for two spin-equilibria systems: ○, low to high; ▽ high to low; ———, $[Fe(pyim)_3](ClO_4)_2$; – – –, $[Fe(pyben)_3](ClO_4)_2$ [65].

expansion in the $^1A_1 \rightarrow {}^5T_2$ activation step is more or less compensated by a solvent contribution of opposite sign. As the numerical values of $\Delta V_{15}^{\neq}$ are in the range 0–9 cm^3 mol^{-1} and as $\Delta V_{51}^{\neq}$ remains constant at about -5 cm^3 mol^{-1}, the solvent and the intrinsic contribution to $\Delta V_{15}^{\neq}$ can be estimated at about -5 cm^3 mol^{-1} and $+9$ cm^3 mol^{-1} respectively (assuming $\Delta V^0 = \Delta V_{15}^{\neq} - \Delta V_{51}^{\neq}$ is about 10 cm^3 mol^{-1}). Thus the intrinsic difference between the quintet ($t_{2g}^4 e_g^2$) and the singlet (t_{2g}^6) states is approximately 14 cm^3 mol^{-1}, which reflects the geometric change by transferring two electrons from antibonding (e_g) to non-bonding (t_{2g}) orbitals. The observed magnitude of $\Delta V_{51}^{\neq}$ and $\Delta V_{15}^{\neq}$ indicates that the transition state geometry is intermediate between those of the ^1A and ^5T states.

The fact that ΔV^0 and $\Delta V_{15}^{\neq}$ decrease with an increase in the donor number suggests that the charge distribution in the complex significantly influences the extent of solvation, the $^1A_1$ isomer being less strongly solvated than the transition state and the $^5T_2$ species. This surprising result is attributed to a lowering of the effective charges on the ligands owing to π back-donation from the metal t_{2g} into empty π^* orbitals of the ligand in the ^1A state (see Fig. 21). For the high-spin case, where the oxygen donor properties are prevalent, the positive charge on the hydrogen atoms close to the surface of the ion will attract polar solvent molecules.

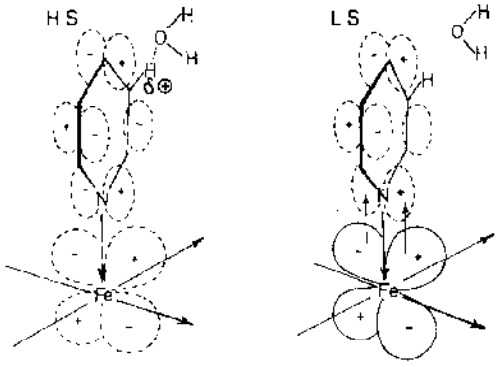

Fig. 21. Schematic drawing showing how the σ-donor and π-acceptor properties of pyridine influence the charge distribution in high-spin and low-spin iron(II) complexes [18].

We shall now briefly comment on the predictions made by the theory of Jortner and coworkers, in which the spin-change processes are described in terms of radiationless multiphoton processes occurring between the two spin states [56]. Also in this scheme the spin conversion is assumed to be non-adiabatic. The justification for this assumption should be that the electronic matrix element connecting the two states **V** is small compared with some characteristic energy parameters representing the nuclear movement. These parameters can be chosen as the metal–ligand vibrational quantum $\hbar\omega$ and the characteristic solvent frequencies $\hbar\omega_s$.

The only term which has non-vanishing spin–orbit coupling matrix elements with both $^1A_1$ and $^5T_2$ is the $^3T_{1g}$ term of the intermediate electronic configuration $t_{2g}{}^5e_g$. Jortner and coworkers have estimated **V** to be 170 cm^{-1} for iron(II) [56]. This value is obtained under the assumption that both spin states have perfect octahedral symmetry and that the free ion values for B and ζ can be used. This is far from the real situation for the system in Table 9. We have made a more realistic calculation using the angular overlap model and structural data from the actual crystal structure of $[Fe(tpen)](ClO_4)_2$. Our estimate for **V** is 270 cm^{-1}, which is nearly double the value of Jortner and coworkers.

The rates predicted by Jortner and coworkers' theory are a few orders of magnitude too high if their estimate of **V** is used. However, use of the more realistic estimate brings the discrepancy up to several orders of magnitude, at the same time as some of the basic assumptions in the model become doubtful.

A consequence of Jortner and coworkers' model is that the quantum tunnelling effect is important, especially at low temperature. Xie and Hendrickson [54,66] have recently shown that tunnelling is indeed observed

for the iron(II) spin-equilibrium system $[Fe(mepy)(py)_2tren](ClO_4)_2$ diluted into a film of sulphonated polystyrene. In the range 300–140 K an apparent activation energy of 15.7 kJ mol^{-1} (acetonitrile) is observed, but below 120 K the relaxation becomes relatively independent of temperature.

The question about how the molecular mechanism of the spin change mechanism occurs can only be answered through a study of a series of carefully designed systems. Valuable information might be obtained from a study of systems, which, because of some steric constraints, can only follow some particular reaction coordinates. A pseudorotational twist movement might, for example, be more favourable than a radial expansion for a cage complex.

Among the systems in Table 9, $[Fe(tpchxn)]^{2+}$ is remarkable because of the restrictions the cyclohexane ring puts on the twist movements this molecule can perform. It is very interesting that this complex is the only one for which a positive $\Delta V_{51}^{\neq}$ has been observed. This result suggests that this particular complex is the only one for which the high-spin, low-spin change occurs via a dissociative mechanism. It is tempting to postulate that the reason for this is the blocking of a more favourable path.

Purcell [69] has suggested that a synchronous enantiomerization and a spin-state isomerization are energetically favourable via a pseudorotational mechanism in which the intermediate is of triplet multiplicity and of trigonal prismatic geometry. We shall now present some of our own results which support this conclusion.

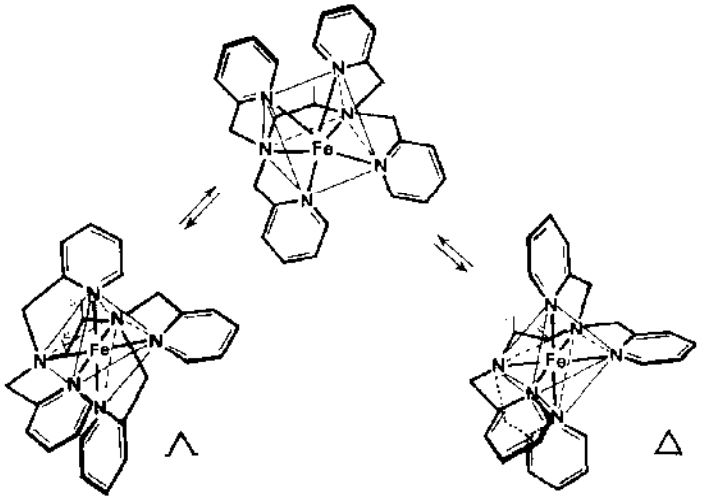

Fig. 22. Change in configuration along a rhombic twist coordinate for $[Fe(tpen)]^{2+}$ [17].

We have used the structural data for $[Fe(tpen)](ClO_4)_2 \cdot H_2O$ [16] as a starting point in an AOM calculation, with the aim of estimating the energetic effects of the distortions in an FeN_6 chromophore. Realizing that the strain-free coordination of the ligand is the trigonal prismatic geometry, we were particularly interested in following the energetic consequences of the transformation from a trigonal prismatic geometry to an octahedral geometry. When the ligand is a hexadentate ligand of the tpen type, this transformation is a pseudorotation, where one py_2N face in the polyhedron is rotated with respect to the other py_2N face, the so-called Rây–Dutt twist or rhombic twist. The transformation can be described in terms of the angle by which the py_2N faces are rotated around the FeN axis. The C_2 axis through the midpoint of the aliphatic chelate ring is preserved during the

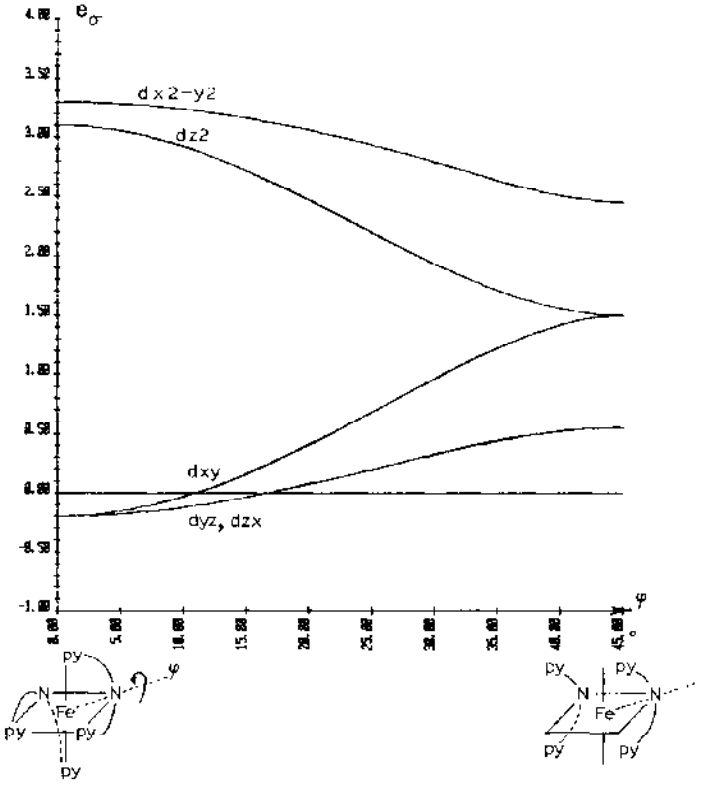

Fig. 23. AOM orbital energies (in units of e_σ) as a function of the twist angle ϕ for $[Fe(tpen)]^{2+}$ [17].

pseudorotation. Only for the trigonal prismatic intermediate is the symmetry C_{2v} (Fig. 22).

In the actual structure of the iron(II) complex the coordinating atoms are arranged nearly octahedrally around the iron; therefore in the calculation we use the e_σ parameter of 5770 cm^{-1} appropriate for $[Fe(tpen)]^{2+}$ [13]. We have chosen the e_π parameter to be $-0.1e_\sigma$. The angular variation of the orbital energies is shown in Fig. 23. The accidental degeneracy for the trigonal prismatic structure should be noted.

Purcell [69] presents a similar calculation, and he has also calculated the angular variation of the term energies. His calculations suggest a crossing of the $^1A_1$ and the ^5A terms about midway along the pseudorotational coordinate. However, the picture should be modified somewhat owing to the pronounced drop in e_σ on going from low spin to high spin. We have estimated this change to be about 40%. We suggest that the pseudorotational and radial movements are synchronous. Furthermore, we expect the spin-state isomerization and the enantiomerization to happen along the same coordinate. However, to reach the spin cross-point, only a fraction of the full pseudorotation is needed.

If the spin change and the racemization have a common reaction coordinate, an unusuallly high racemization rate for iron(II) spin-equilibria systems is expected.

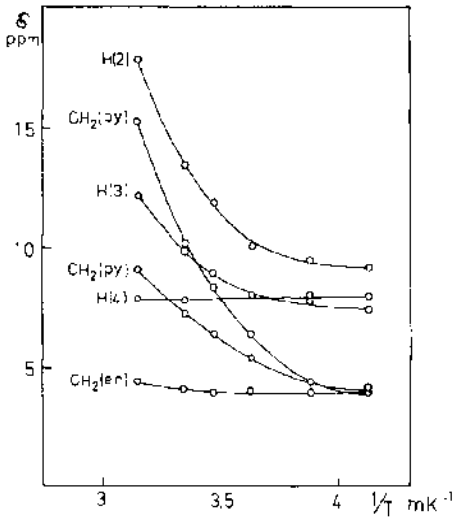

Fig. 24. Temperature variation of the ^1H NMR chemical shifts for $[Fe(tpen)]I_2$ in a water–methanol (1 : 1 v/v) mixture [16].

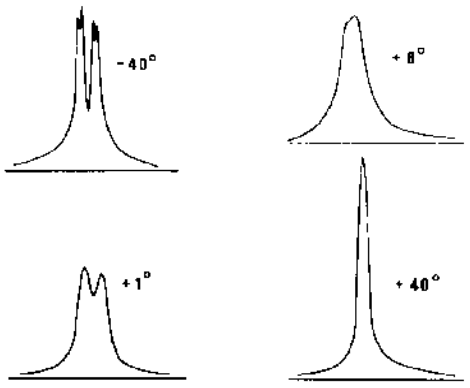

Fig. 25. The CH_3 ^1H NMR spectrum of $[Fe(tpmbn)](ClO_4)_2$ in acetone at four different temperatures [17].

Variable-temperature ^1H and ^{13}C NMR spectra have been reported for a few spin-equilibria complexes [49,50], but they do not give direct information about the spin change rate because these rates exceed what can be followed by the NMR technique. However, other valuable dynamic information can be extracted from these experiments.

In Fig. 24 the temperature variation of the chemical shifts for $[Fe(tpen)]I_2$ in a water–methanol mixture is shown. In the temperature range covered (-31 to $45\,^\circ C$), the high-spin fractions are changed from 0.003 to 0.10. Very surprisingly the number of lines, even for the lowest temperatures, suggests that the molecule is fluxional. The separation between non-equivalent protons in one of the enantiomers of $[Fe(tpchxn)]^{2+}$ is known to be of the order of magnitude 14 Hz, so that even at $-31\,^\circ C$ the rate constant for the racemization in $[Fe(tpen)]^{2+}$ exceeds 600 s^{-1}.

In the case of $[Fe(tpmbn)]^{2+}$ the enantiomerization in acetone solution has been followed by the temperature variation of the chemical exchange of the CH_3 groups (Fig. 25). The racemization rate constant at 273 K was found to be 156 s^{-1}, which is six orders of magnitude greater than that for the same reaction in the low-spin complex $[Fe(tptcn)]^{2+}$ [68]. Rapid racemization has also been observed for the $[Fe(phen)_3]^{2+}$ system [23].

A pseudorotational mechanism for the racemization of these iron(II) complexes is the most plausible possibility, since the rates of the ligand dissociations have been shown to be much slower [18].

F. CONCLUSIONS

As a conclusion we have found that it is possible to design new spin-equilibria systems through carefully planned ligand synthesis. A system having a

critical ligand field strength will in general show the spin-equilibrium phenomenon in the solid as well as in solution. The value of the observed critical temperature T_c for a given system depends on the nature of the counter-ion, the solvent and the crystal packing. The spin change is always accompanied by geometrical changes in the ligand sphere around the metal ion. These changes are observed both in the metal ligand distance and in the angular twist movements of the coordination polyhedron.

The spin change rates are generally so high that they will never become rate-determining steps in more complex reactions, e.g. in intermolecular electron transfer reactions.

The light-induced spin-state conversion observed in some systems opens the possibility of the construction of advanced optical materials. If the spin-state trapping can be achieved at room temperature, materials for optical data storage might be obtained. However, the construction of optical components based on the non-linear optical properties of the materials offers a more realistic application, e.g. as an optical switch.

REFERENCES

1 K. Madeja and E. König, J. Inorg. Nucl. Chem., 25 (1963) 377.
2 L.E. Orgel, Quelques Problèmes de Chimie Minerales, 10ème Conseil de Chimie, Bruxelles, 1956, p. 289.
3 R.L. Martin and A.H. White, Transition Met. Chem., 4 (1968) 113.
4 L. Sacconi, Pure Appl. Chem., 27 (1971) 161.
5 H.A. Goodwin, Coord. Chem. Rev., 18 (1976) 293.
6 P. Gütlich, Struct. Bonding (Berlin), 44 (1981) 83.
7 E. König, G. Ritter and S.K. Kulshreshtha, Chem. Rev., 85 (1985) 219.
8 C.K. Jørgensen, Modern Aspects of Ligand Field Theory, North Holland, Amsterdam, 1971, p. 347.
9 A.T. Baker and H.A. Goodwin, Aust. J. Chem., 37 (1984) 1157.
10 R.D. Hancock and G.J. McDougall, J. Chem. Soc., Dalton Trans., (1977) 67.
11 L. Christiansen and H. Toftlund, in J. Avery, J.P. Dahl and Å. Hansen (Eds.), Understanding Molecular Properties, Reidel, Dordrecht, 1987, p. 177.
12 S.M. Nelson and J. Rodgers, J. Chem. Soc. A, (1968) 272.
13 H. Toftlund and S. Yde-Andersen, Acta Chem. Scand., Ser. A, 35 (1981) 575.
14 G. Anderegg and F. Wenk, Helv. Chim. Acta, 50 (1967) 2330; Chimia, 24 (1970) 427.
15 R.K. Boggess, J.W. Hughes and C.W. Chew, J. Inorg. Nucl. Chem., 43 (1981) 939.
16 H.R. Chang, D.N. Hendrickson, J. Hvam, H. Toftlund, A.X. Trautwein, S.R. Wilson and H. Winkler, Inorg. Chem., to be published.
17 J.J. McGarvey, I. Lawters, K. Heremans and H. Toftlund, Inorg. Chem., to be published.
18 H. Toftlund, unpublished results.
19 L.J. Wilson, D. Georges and M.A. Hoselton, Inorg. Chem., 14 (1975) 2968.
20 A.M. Greenaway, C.J. O'Connor, A. Schrock and E. Sinn, Inorg. Chem., 18 (1979) 2692.
21 M. Sorai, J. Ensling, K.M. Hasselbach and P. Gütlich, J. Chem. Phys., 20 (1977) 197.
22 M. Sorai, J. Ensling and P. Gütlich, J. Chem. Phys., 18 (1976) 199.

23 L. Christiansen, D.N. Hendrickson, H. Toftlund, S.R. Wilson and C.-L. Xie, Inorg. Chem., 25 (1986) 2813.
24 F. Højland, H. Toftlund and S. Yde-Andersen, Acta Chem. Scand., Ser. A, 37 (1983) 251.
25 H. Toftlund, E. Pedersen and S. Yde-Andersen, Acta Chem. Scand., Ser. A, 38 (1984) 693.
26 E. König, G. Ritter, J. Dengler and S.M. Nelson, Inorg. Chem., 26 (1987) 3582.
27 H.A. Goodwin and K.H. Sugiyarto, Chem. Phys. Lett., 139 (1987) 470.
28 E. König and K. Madeja, Spectochim. Acta, 23 (1967) 45.
29 H. Winkler, A. Sawaryn, A.X. Trautwein, A.A. Yousif, C. Hermos, H. Toftlund and R.H. Herber, Hyperfine Interactions, to be published.
30 J. Fleisch, P. Gütlich, K. Hasselbach and F.W. Müller, Inorg. Chem., 15 (1976) 958.
31 Y. Maeda and Y. Takashima, Comments Inorg. Chem., (1988) to be published.
32 E. Bill, A.X. Trautwein, H. Winkler and H. Toftlund in A. Xavier (Ed.), Frontiers in Bioinorganic Chemistry, VCH Verlag, Berlin, 1986, p. 507.
33 H. Winkler, Stochastic Model for Dynamic Hyperfine Interactions, Habilitationsschrift, Hamburg, 1983.
34 (a) P. Adler, H. Spiering and P. Gütlich, Hyperfine Interactions, to be published.
(b) P. Adler, Untersuchung der Dynamik des High Spin ($^5T_{2g}$) Low Spin ($^1A_{1g}$) Intersystem Crossing in Eisen(II)-Komplexen durch Linienformanalyse von Mössbauer-Spektren, Dissertation, Mainz, 1988.
35 P. Adler, H. Spiering and P. Gütlich, Inorg. Chem., 26 (1987) 3840.
36 A. Hauser, P. Gütlich and H. Spiering, Inorg. Chem., 25 (1986) 4245.
37 E. König and K. Madeja, J. Chem. Soc., Chem. Commun., 3 (1966) 61.
38 B.A. Katz and C.E. Strouse, J. Am. Chem. Soc., 101 (1979) 6214.
39 L. Wiehl, G. Kiel, C.P. Köhler, H. Spiering and P. Gütlich, Inorg. Chem., 25 (1986) 1565.
40 E. König, Prog. Inorg. Chem., 35 (1987) 527.
41 K.B. Jensen, S. Oshio and H. Toftlund, Inorg. Chem., to be published.
42 D.L. Kepert, Inorganic Stereochemistry, Springer, New York, 1982.
43 J. Gladstone, N.J. Rose and E.C. Lingafelter, Inorg. Chem., 25 (1986) 1516.
44 B.A. Katz and C.E. Strouse, Inorg. Chem., 19 (1980) 658.
45 K. Wieghardt, E. Schöffmann, B. Nuber and J. Weiss, Inorg. Chem., 25 (1986) 4877.
46 J.D. Oliver, D.F. Mullica, B.B. Hutchinson and W.O. Milligan, Inorg. Chem., 19 (1980) 165.
47 H.L. Chum, J.A. Vanin and M.I.D. Holanda, Inorg. Chem., 21 (1982) 1146.
48 P.H. van der Voort and W.L. Driessen, Proc. 16th Int. Conf. Coord. Chem., Dublin, 1974. R43.
49 J.P. Jesson, S. Trofimenko and D.R. Eaton, J. Am. Chem. Soc., 89 (1967) 3158.
50 M.A. Hoselton, L.J. Wilson and R.S. Drago, J. Am. Chem. Soc., 97 (1975) 1722.
51 L.L. Martin, R.L. Martin, K.S. Hagen, A. Hauser and A. Sargeson, J. Chem. Soc., Chem. Commun., (1988) 1313.
52 W. Levason, C.A. McAuliffe, M.M. Mahfooz and S.M. Nelson, J. Chem. Soc., Dalton Trans., (1975) 1778.
53 K.A. Reeder, E.V. Dose and L.J. Wilson, Inorg. Chem., 17 (1978) 1107.
54 A.J. Conti, C.-L. Xie and D.N. Hendrickson, J. Am. Chem. Soc., to be published.
55 (a) M. Bacci, Coord. Chem. Rev., 86 (1988) 245.
(b) J.K. Beattie, Adv. Inorg. Chem., 32 (1988) 1.
56 E. Buhks, G. Navon, M. Bixon and J. Jortner, J. Am. Chem. Soc., 102 (1980) 2918.
57 E.V. Dose, M.A. Hoselton, N. Sutin, M.F. Tweedle and L.J. Wilson, J. Am. Chem. Soc., 100 (1978) 1141.
58 J.K. Beattie, N. Sutin, D.H. Turner and G.W. Flynn, J. Am. Chem. Soc., 95 (1973) 2052.

59 J.K. Beattie, R.A. Binstead and R.J. West, J. Am. Chem. Soc., 100 (1978) 3044.
60 M.A. Hoselton, R.S. Drago, L.J. Wilson and N. Sutin, J. Am. Chem. Soc., 98 (1976) 6967.
61 E.V. Dose, K.M.M. Murphy and L.J. Wilson, Inorg. Chem., 15 (1976) 2622.
62 R.H. Petty, E.V. Dose, M.F. Tweedle and L.J. Wilson, Inorg. Chem., 17 (1978) 1064.
63 M.F. Tweedle and L.J. Wilson, J. Am. Chem. Soc., 98 (1976) 4824.
64 J.J. McGarvey and I. Lawthers, J. Chem. Soc., Chem. Commun., (1982) 904.
65 J.J. McGarvey, I. Lawthers, K. Heremanns and H. Toftlund, J. Chem. Soc., Chem. Commun., (1984) 1575.
66 C.-L. Xie and D.N. Hendrickson, J. Am. Chem. Soc., 109 (1987) 6981.
67 V. Gutmann, Electrochim. Acta, 21 (1976) 661.
68 G.A. Lawrance and D. Stranks, Inorg. Chem., 17 (1978) 1804.
69 K.F. Purcell, J. Am. Chem. Soc., 101 (1979) 5147.
70 J. DiBenedetto, V. Arkle, H.A. Goodwin and P.C. Ford, Inorg. Chem., 24 (1985) 455.